PNNL-17387

Smolt Responses to Hydrodynamic Conditions in Forebay Flow Nets of Surface Flow Outlets, 2007

DRAFT FINAL REPORT
June 30, 2008

Prepared for:
U.S. Army Corps of Engineers, Portland District
Under an Interagency Agreement with
the U.S. Department of Energy
Contract DE-AC05-76RLO 1830

Prepared by:
Pacific Northwest National Laboratory
Tenera Environmental, Inc.

DISCLAIMER

PACIFIC NORTHWEST NATIONAL LABORATORY
operated by
BATTELLE
for the

UNITED STATES DEPARTMENT OF ENERGY

under Contract DE-AC05-76RL01830

PNNL-17387

Smolt Responses to Hydrodynamic Conditions in Forebay Flow Nets of Surface Flow Outlets, 2007

GE Johnson
MC Richmond
JB Hedgepeth[a]
GR Ploskey
MG Anderson
Z Deng
F Khan
RP Mueller
CL Rakowski
NK Sather
JA Serkowski
JR Steinbeck[a]

DRAFT FINAL REPORT
June 30, 2008

Prepared for the U.S. Army Corps of Engineers
Portland District, Portland, Oregon
under a Related Services Agreement
with the U.S. Department of Energy
Contract DE-AC05-76RL01830

Pacific Northwest National Laboratory, Richland, Washington
[a] Tenera Environmental, San Luis Obispo, California

Executive Summary

This study provides information on juvenile salmonid behaviors at McNary and The Dalles dams that can be used by the U.S. Army Corps of Engineers, fisheries resource managers, and others to support decisions on long-term measures to enhance fish passage. The goal of the study was to use fish behavioral responses to ambient flow fields to support general design guidelines for hydraulic conditions that readily pass juvenile salmon at surface flow outlets. The study is also applicable to bioengineering for juvenile salmonid passage at irrigation diversions, tide gates, and culverts. We integrated data on smolt movements and hydrodynamic conditions at SFOs at McNary and The Dalles dams during 2007 to address the following questions:

- Which hydraulic variables are most strongly associated with fish behavioral responses?
- Of these, are there threshold levels that could be used to support SFO design guidelines?

Objectives

We collected data during April 21-26, 2007 at McNary Dam and May 1 to July 12, 2007 at The Dalles Dam. The research objectives were: McNary Dam -- Conduct a pilot study of simultaneous fish behavior and water velocity data in the nearfield (< 20 m) of a prototype Temporary Spillway Weir (TSW) to:

1. Establish a deployment procedure and collect preliminary data.
2. Assess the feasibility of this technique to study smolt responses to hydrodynamics at a McNary TSW (No. 2).

The Dalles Dam -- Apply new empirical data from simultaneous remote sensing techniques and computational fluid dynamics modeling in the nearfield of the sluiceway to:

1. Characterize fish behavior and water velocity patterns.
2. Examine descriptive and statistical associations between juvenile salmonid movements and hydrodynamic conditions immediately upstream of the SFO entrances.
3. Address guidelines for hydraulic parameters of the flow net upstream of this SFO that would be conducive to juvenile salmonids passing into the SFO entrance.

Approach

In the field, we collected simultaneous data from an acoustic Doppler current profiler (ADCP) and a dual-frequency identification sonar (DIDSON). The ADCP and DIDSON acoustic beams were oriented to sample overlapping water volumes. At McNary Dam, the equipment was deployed upstream of the TSW at Bay 19. At The Dalles Dam, the instruments were deployed upstream off the face of the dam to sample in the nearfield (< 20 m) of Sluices 1-1 and 1-2 during six 4-day sampling episodes. The main drawback of the ADCP, however, is that the size of its sample volume can be large (meters) relative to the size of the fish (centimeters); this factor increases as range increases. Therefore, we supplemented the study at The Dalles with CFD modeling for a scenario with

consistent dam operations in the vicinity (MU1-4) of the DIDSON sample volume. The CFD allowed fine-scale spatial resolution, but was steady-state temporally. We merged the water and fish data sets to calculate the fish effort variables (Figure ES.1) that are elemental to this study.

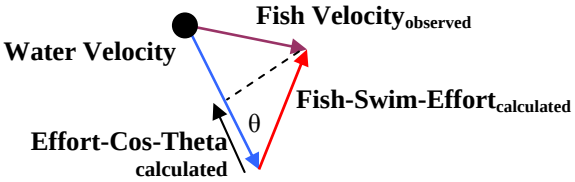

Figure ES.1. Observed and calculated fish variables get at the heart of the matter. The water velocity vector can be obtained from ADCP or CFD data. Observed fish movement, as measured from the DIDSON images, is the result of the interaction between the flow field, as measured with the ADCP or simulated with the CFD, and fish swimming behavior. The main dependent variables used in subsequent analyses were fish-swim-effort (m/s) and effort-cos-theta (m/s).

Comparison of the ADCP and CFD results revealed an apparent problem with our application of the ADCP. The instrument was functioning properly, but the assumption that water currents were sufficiently homogenous for a given range in the ADCP beams may not have been met, producing anomalous water velocity vectors. We plan to delve deeper into the issue in collaboration with the instrument vendor. In the meantime, all water-related and fish effort variables were calculated using CFD data.

Results

Computational fluid dynamics data show the oblique flow into the sluiceway at The Dalles dam (Figure ES.2). Flow abruptly accelerates inside the piers and over the sill at the sluiceway entrances.

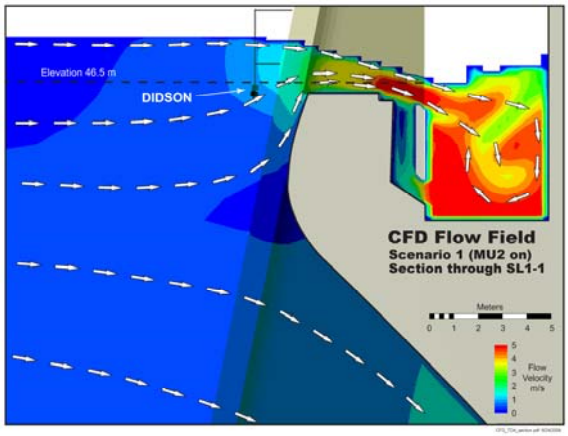

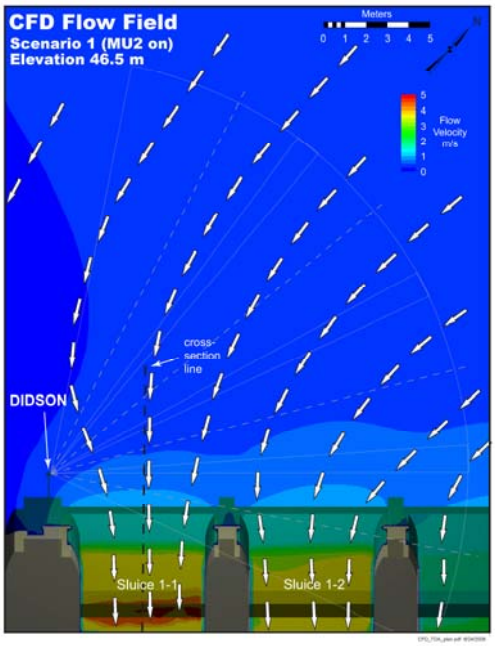

Figure ES.2. CFD results show abruptly changing flow into the sluiceway at The Dalles Dam, El. 158.5 ft. Total discharge 273, spillway 110, powerhouse 163 kcfs. Sluice 1-1 and 1-2 2.7, MU1 9.9 and MU2 9.8 kcfs.

Fish swimming relative to flow, based on effort-cosine-theta to categorize fish behaviors, was: a) passive, b) active swimming against the flow (positive rheotaxis), and c) active swimming with the flow (negative rheotaxis). Passive behavior was defined as being within 0.03 m/s of zero, i.e., about one-fifth of a body length per second. The majority behavior was active swimming against the flow (65-85%) (Figure ES.3). Conversely, approximately 10-30% of the behavior at The Dalles Dam was active swimming with the flow (negative rheotaxis). A small fraction of swimming behavior was passive (~5%). Swimming against the flow (positive rheotaxis) was more common in summer than spring at The Dalles Dam. Generally, individual fish were less likely to swim against the flow than schools of fish.

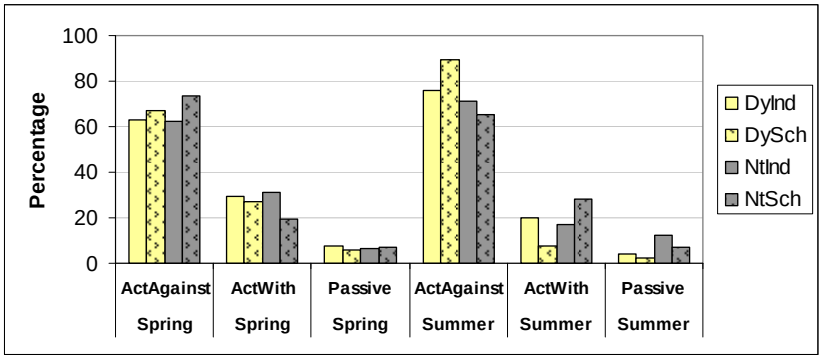

Figure ES.3. The most common fish behavior relative to flow was actively swimming against the flow. Percentages based on effort-cos-theta were calculated seasonally for individual fish and schools during day and night separately, e.g., for spring/day/individuals, the sum of percentages for active against, active with, and passive equals 100.

Fish effort superimposed on flow conditions shows relatively high fish-swim-effort values and negative effort-cos-theta just upstream of the sluice entrances (Figure ES.4). Water velocity increases in this region, as does acceleration and strain.

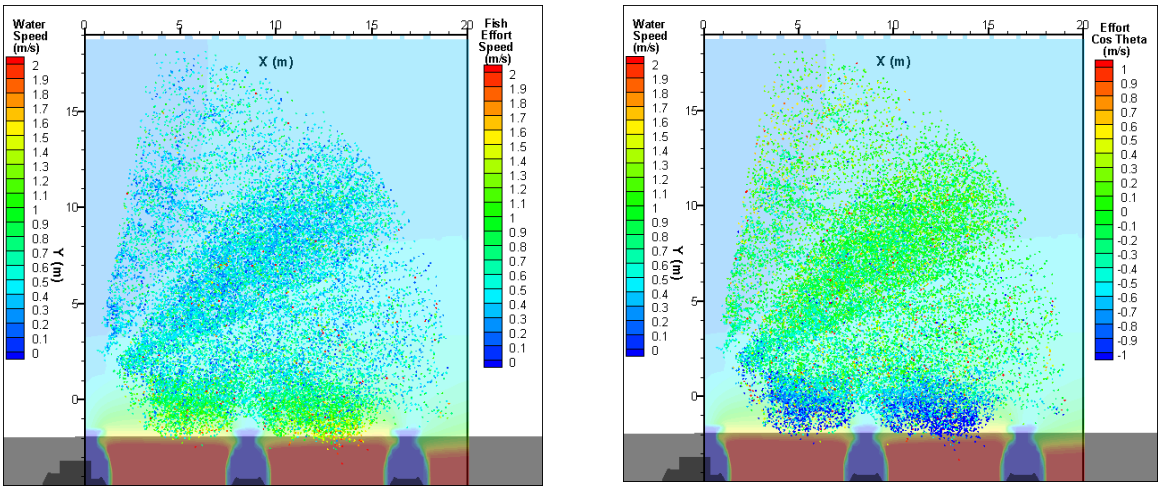

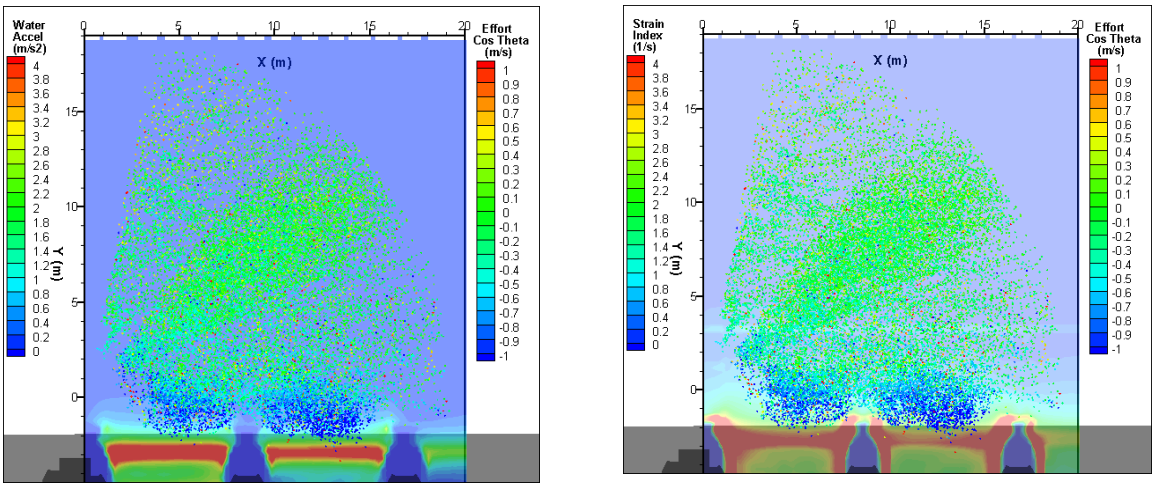

Figure ES.4. Fish-swim-effort and effort-cos-theta are associated with water velocity fields (top row), acceleration field (bottom left), and strain field (bottom right). Hydraulic data are from the CFD simulation. The fish data points are ping-to-ping observations processed from DIDSON output.

A *correlation analysis* shows that effort-cos-theta had higher correlations with hydraulic variables than did fish-swim-effort (Table ES.1). The highest correlations (0.46-0.47) were between effort-cos-theta and water velocity magnitude, V (water velocity y-component, perpendicular to the dam), W (water velocity vertical-component), total acceleration, and strain. Most of spatial derivatives of velocity were not strongly correlated with the fish behavior variables.

Table ES.1. Correlation Matrices between Fish Behavior and CFD Hydraulic Variables for All Data Combined for The Dalles Dam. See the report for definitions of variables. Cells with correlation coefficients greater than 0.4 are shaded to ease examination of the table. There were 22,878 data points for each Pearson correlation.

	U	V	W	VelocityMag.	dUdX	dVdX	dWdX	dUdY	dVdY	dWdY
Xeffort	0.04	-0.17	0.16	0.17	-0.13	0.08	-0.06	0.08	0.15	-0.14
Yeffort	0.06	-0.41	0.41	0.41	-0.29	0.07	-0.16	0.12	0.36	-0.37
Fish-Swim-Effort	0.03	-0.36	0.36	0.36	-0.26	0.09	-0.16	0.12	0.33	-0.32
Effort-Cos-Theta	-0.19	0.47	-0.47	-0.46	0.36	-0.04	0.13	-0.10	-0.42	0.42

	dUdZ	dVdZ	dWdZ	AU	AV	AZ	Total Accel.	Strain
Xeffort	0.05	-0.15	-0.16	-0.05	-0.14	0.12	0.15	0.17
Yeffort	0.17	-0.38	-0.39	-0.02	-0.34	0.32	0.34	0.39
Fish-Swim-Effort	0.13	-0.35	-0.35	-0.03	-0.32	0.28	0.32	0.35
Effort-Cos-Theta	-0.26	0.43	0.44	0.00	0.37	-0.37	-0.38	-0.46

A *non-linear regression analysis* was applied to examine quantitative relationships between the fish behavior variables and hydraulic variables to assess its usefulness to support development of SFO design guidelines. For fish-swim-effort and effort-cos-theta as the dependent variables (Figure ES.5), the scatter cloud of data points was oriented in upward and downward directions, respectively, as the independent variable increased from its low values during both spring and summer. The corresponding splines reflected this as fish-swim-effort and effort-cos-theta trended upward and

downward, respectively, as velocity, acceleration, or strain increased. As an example, during spring effort-cos-theta peaked at approximate velocity 0.9 m/s, acceleration 0.25 m/s^2, and strain 0.95 s^{-1}. Note, the data were sparse at the high end for all independent variables.

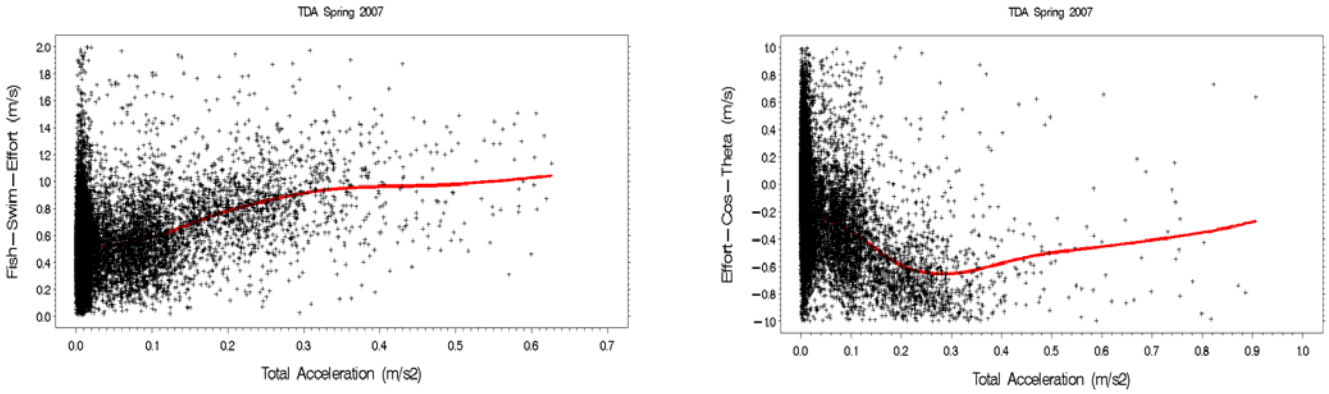

Figure ES.5. Example fish/flow relationships indicate the potential for empirically-based design guidelines. Leveling of the effort variables could indicate a response threshold. Data are for The Dalles Dam, spring 2007, fish swimming effort (left) and effort-cosine-theta (right) vs. total acceleration.

Management Implications

The new information the 2007 results provide has management implications:

1. Schooling behavior was dynamic and prevalent. The implication is that SFO entrance area must be large enough to accommodate fish schools.
2. Fish behavior was dependent on distance from the SFO entrance. This supports the notion that SFO flow nets need to be expansive enough spatially to attract smolts despite competing flow fields.
3. Passive fish behavior was observed less than 5% of the time in the SFO flow nets we studied, implying that SFO designs cannot rely only on fish following bulk flow.
4. Active swimming against the flow was the most common behavioral response. SFO performance evaluations should include a metric for fish swimming effort in SFO flow fields.
5. Fish effort variables were correlated with water velocity, acceleration, and strain. The non-linear regressions indicate potential for this approach of merging fish/flow data to lead to SFO design guidelines in the future as the fish/flow dataset is further populated.

Conclusion

Analyzing merged fish/flow data from a diversity of sites in multiple years will strengthen the relationships between smolt responses and hydrodynamic conditions such that universal trends may emerge to support bioengineering efforts aimed at protecting juvenile salmonids.

Preface

This research was conducted under the auspices of the U.S. Army Corps of Engineers, Northwestern Division's Anadromous Fish Evaluation Program (AFEP) to implement the Congressionally-appropriated Columbia River Fish Mitigation project. The research pertains to AFEP study codes SBC-W-06-01 and SBE-P-00-17. It was funded by the U.S. Army Corps of Engineers (USACE) Portland and Walla Walla Districts under a contract with the Pacific Northwest National Laboratory (PNNL), operated by Battelle for the U.S. Department of Energy. Tenera Environmental, Inc. was a subcontractor to PNNL.

Analysis and reporting for this study had three successive phases. First, descriptive data and DIDSON videos reported at the AFEP Annual Review in December 2007 showed high resolution, fine-scale fish movements at SFO entrances. Second, we merged the water and fish data sets to calculate the fish effort variables that are the foundation of this study; preliminary results were released at a SRWG meeting on March 27, 2008. Third, CFD results were incorporated into the analysis and are reported herein.

Acknowledgments

We gratefully acknowledge contributions to this study by:

- Honald Crane Services – Bob Austin and Mike Honald;
- PNNL staff –Dennis Dauble, Eric Fischer, David Geist, Terri Gilbride, James Hughes, Julie Hughes, Kathy Lavender, Mark Weiland, and Shon Zimmerman;
- Schlosser Machine Shop - Vincent Schlosser;
- U.S. Army Corps of Engineers fisheries biologists – Bob Cordie, Brad Eby, Mike Langeslay, Ann Setter, Bob Wertheimer, and Miro Zyndol;
- U.S. Army Corps of Engineers personnel – Ryan Bliss, Laurie Ebner, Dick Harrison, Lance Helwig, Art Kunigel, and Lynn Reese.

Contents

Executive Summary i

Preface vii

Acknowledgments vii

1.0 Introduction 1.1

1.1 Background 1.1

1.2 Objectives 1.4

1.3 Report Content 1.4

2.0 Methods 2.1

2.1 General Approach 2.1

2.2 Field Data Collection 2.2
2.2.1 ADCP 2.2
2.2.2 DIDSON 2.4
2.2.3 Sampling Locations and Orientations 2.5
2.2.4 Sampling Schedule and Environmental Conditions 2.6

2.3 Computational Fluid Dynamics Modeling 2.9

2.4 Data Processing and Analysis 2.10
2.4.1 Subsample Data Set 2.10
2.4.2 Variables 2.11
2.4.3 Processing and Analysis Methods 2.13

3.0 Results 3.1

3.1 Water Velocity 3.1

3.2 Fish Observations 3.4
3.2.1 Visualizations 3.4
3.2.2 Movement Tallies 3.5
3.2.3 Fish Speeds 3.8

3.3 Fish Behavior Relative to Hydrodynamics 3.10
3.3.1 Fish Swimming Behavior Relative to Flow 3.10
3.3.2 Correlation Analysis 3.12
3.3.3 Non-Linear Regression Analysis 3.14

4.0 Discussion 4.1

5.0 Literature Cited 5.1

Appendix A Data Processing and Analysis Methods A.1

A.1 Data Processing A.1
A.1.1 ADCP A.1

A.1.2 DIDSON A.4
A.1.3 CFD A.5
A.1.4 Merging A.5
A.1.5 Observation Visualization A.7
A.2 Data Analysis A.7
A.2.1 Data Filters A.7
A.2.2 Fish Behavior Tallies A.7
A.2.3 Non-Linear Regression Analysis A.7

Figures

Figure 1.1. Map of U.S. Dams on the Columbia and Snake Rivers. Dots and circles signify dams with a full production SFO or an SFO under development, respectively. Modified from a map obtained at //www.nwcouncil.org/. 1.1
Figure 2.1. ADCP/DIDSON 2.1
Figure 2.2. Sample Volume -- Side View of Simultaneous ADCP (red) and DIDSON (purple) Acoustic Beams. The background is The Dalles Dam powerhouse. In this schematic, the DIDSON was aimed across the face of the dam in a northeast direction. 2.1
Figure 2.3. Sample Volume -- Plan View of Simultaneous ADCP (red) and DIDSON (purple) Acoustic Beams. The background is The Dalles Dam powerhouse. The projection of the sloping piers into the beams is an artifact of the graphic. 2.2
Figure 2.4. Photograph of a 600-kHz ADCP (left) and Beam Velocity Schematic (right, after RDI 1996). Cardinal directions given in the right-side figure are for descriptive purposes only, and deployment orientation of the ADCP beams was not specific to any coordinate system. 2.3
Figure 2.5. Plan (left) and Side (right) Views Showing ADCP and DIDSON Instrument Location and Sample Volumes Relative to TSW 2 at McNary Dam, 2007 ..... 2.5
Figure 2.6. Photographs of ADCP/DIDSON Deployment at McNary Dam, 2007 ..... 2.5
Figure 2.7. Plan View Showing ADCP and DIDSON Instrument Location and Sample Volumes Relative to the Sluiceway at The Dalles Dam, 2007 ..... 2.6
Figure 2.8. Photograph of the ADCP/DIDSON at The Dalles Dam, 2007 ..... 2.6
Figure 2.9. Run Timing at McNary Dam, 2007. Data are from Data Access in RealTime (DART) (http://www.cbr.washington.edu/dart/). 2.7
Figure 2.10. Total River Discharge (1,000 cubic feet per second; kcfs) and Spill Discharge (kcfs) at McNary Dam, Spring 2007. This figure was obtained from DART. 2.7
Figure 2.11. Run Timing at John Day Dam, 2007. Data are from DART. 2.8
Figure 2.12. Total River (Outflow) and Spill Discharge (kcfs) during Spring and Summer 2007 at The Dalles Dam. The figure was obtained from DART. 2.8
Figure 3.1. Sectional (top) and Plan (bottom) Views of the Simulated Velocity Field for a Single-bay CFD Model of the TSW at McNary Dam. Forebay elevation 340 ft MSL. TSW discharge 10.7 kcfs. 3.2
Figure 3.2. Sectional (top) and Plan (bottom) Views of the Simulated Velocity Field Near the Sluiceway Entrance SL 1-1 and SL 1-2 at Main Unit 1 at The Dalles Dam for Flow Scenario 1 (Table 2.2). 3.3

Figure 3.3. Plan View Visualization of Fish Events during Day, Spring 2007, McNary Dam (left) and The Dalles Dam (right). Blue = single fish; green = 3 to 10 fish; red >10 fish..... 3.5
Figure 3.4. Schooling Behavior. Expressed as a percentage of total schools and individuals observed with the DIDSON and calculated separately for day and night during spring and summer at McNary (MCN) and The Dalles (TDA) dams. 3.6
Figure 3.5. Directed Movement Behavior. Expressed as a percentage of total directed and non-directed movement observed with the DIDSON and calculated separately for day and night for each aiming position during spring and summer at McNary (MCN) and The Dalles (TDA) dams. Aiming positions are defined in Figures 2.5 and 2.7. ..... 3.6
Figure 3.6. Movement Paths. Expressed as a percentage of total movement paths observed with the DIDSON and calculated separately for day and night for each aiming position during spring at McNary Dam (A) and spring (B) and summer (C) at The Dalles Dam. The path categories "Left to Right" and "Right to Left" are from the dam looking perpendicular into the forebay. Aiming positions are defined in Figures 2.6 and 2.8..... 3.8
Figure 3.7. Contour and Vector Plots of Observed Fish Speed (m/s)..... 3.9
Figure 3.8. Observed Fish and Water Velocity Vectors and the Calculated Fish Swimming Effort Vector along with Swimming Angle (θ) and Effort-Cosine-Theta. 3.10
Figure 3.9. Box-Whisker Plots of Fish-Swimming-Effort (m/s) and Effort-Cosine-Theta (m/s) for Individual Fish and Schools by Day/Night. Effort cosine theta values above the reference line (> 0 m/s) indicate fish swimming with the flow and vice versa for swimming against the flow. 3.11
Figure 3.10. Fish Behavior Percentages. Behavior categories are passive, active swimming against the flow, and active swimming with the flow. See text for definitions. Percentages were calculated seasonally for separately for individual fish and schools during day and night, e.g., for spring/day/individuals, the sum of percentages for active against, active with, and passive equals 100..... 3.11
Figure 3.11. Fish-swim-effort and effort-cos-theta are associated with water velocity fields (top row), acceleration field (bottom left), and strain field (bottom right). Hydraulic data are from the CFD simulation. The fish data points are ping-to-ping observations processed from DIDSON output. 3.12
Figure 3.12. Scatterplots with Non-Linear Regression Splines for Fish-Swim-Effort versus Water Velocity Magnitude, Total Acceleration, and Strain at The Dalles Dam during Spring and Summer 2007. ..... 3.15
Figure 3.13. Scatterplots with Non-Linear Regression Splines for Effort-Cos-Theta versus Water Velocity Magnitude, Total Acceleration, and Strain at The Dalles Dam during Spring and Summer 2007. ..... 3.16
Figure A.1. The ADCP velocity (U, V, W) and the Dam Coordinate Systems. The inset shows the four individual acoustic beams.....A.1
Figure A..2. Filtering the Root-Mean-Square ADCP Velocity Measurements Using Different Running Averaging Filters.....A.4

Tables

Table 1.1. Research on Fish Movements and Flow Fields in the Anadromous Fish Evaluation Program. 1.3
Table 2.1. Schedule for ADCP/DIDSON Sampling at the Sluiceway at The Dalles Dam. Positions (aiming angles) are shown in Figure 2.7. ..... 2.7
Table 2.2. Hours Processed for the 2007 Data Set. Asterisk (*) indicates only 20 min of data were processed due to large number of fish. 2.10
Table 3.1. Descriptive Statistics for Hydraulic Data from the CFD Model for Scenario 1 (Table 2.2). 3.4
Table 3.2. Numbers of Observations Used in the Analyses 3.5
Table 3.3. Fish Movement Tally Data. Movement variables are defined in Section 2.4.2. The path categories are from the dam looking into the forebay. Aiming positions are in Figures 2.5 and 2.7. Missing periods zero observations. 3.7
Table 3.4. Correlation Matrices between Fish Behavior and CFD Hydraulic Variables for All Data Combined for The Dalles Dam See Section 2.3.2 for variable definitions. Cells with correlation coefficients greater than 0.4 are shaded to ease examination of the table. There were 22,878 data points for each Pearson correlation. 3.13
Table 3.5. Correlation Matrices between Fish Behavior and CFD Hydraulic Variables Separately for Combinations of Spring and Summer, Day and Night, and Individuals and Schools. See Section 2.3.2 for variable definitions. Cells with correlation coefficients greater than 0.4 are shaded to ease examination of the table. There were 22,878 data points for each Pearson correlation. . 3.14
Table A.1. Filters on Event Data. The merged data prior to filtering totaled 50,220 ping observations comprising 4,953 fish events for both dams and seasons combined. A.7

1.0 Introduction

Surface flow outlets (SFO) are the main structural means currently being advocated to protect juvenile salmonids at Columbia-Snake River dams (National Oceanic and Atmospheric Administration 2008; Figure 1.1). However, design guidelines for SFO entrance structures and their forebay flow nets are currently based on professional judgment. Data on smolt responses to hydraulic conditions could lead to structural designs that reduce costs while maintaining high fish passage efficiencies.

During 2007, the U.S. Army Corps of Engineers (USACE) contracted Pacific Northwest National Laboratory (PNNL) to evaluate smolt responses to hydrodynamic conditions at SFOs at McNary and The Dalles dams. The goal of the study was to use fish behavioral responses to ambient flow fields to support general design guidelines for hydraulic conditions that readily pass juvenile salmon at surface flow outlets. The study is also applicable to bioengineering for juvenile salmonid passage at irrigation diversions, tide gates, and culverts.

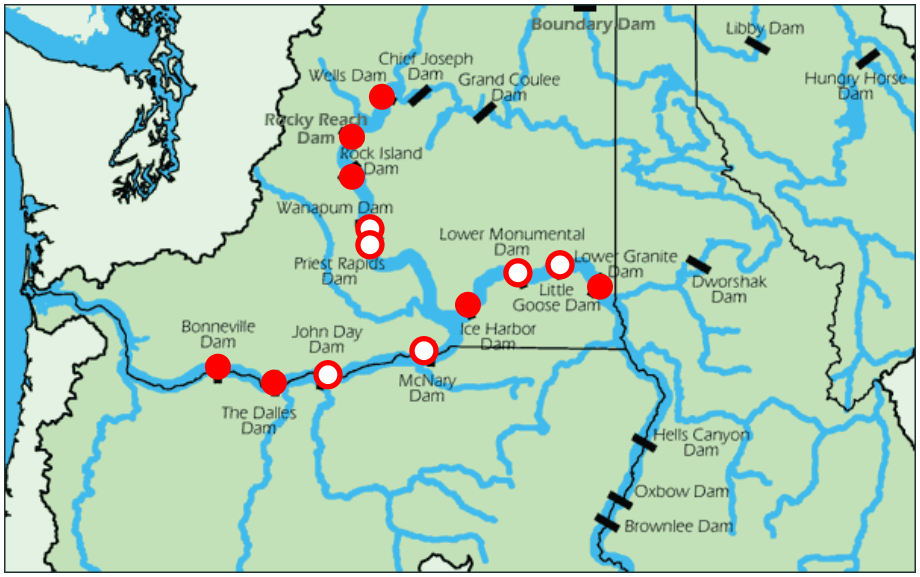

Figure 1.1. Map of U.S. Dams on the Columbia and Snake Rivers. Dots and circles signify dams with a full production SFO or an SFO under development, respectively. Modified from a map obtained at //www.nwcouncil.org/.

1.1 Background

Development of surface routes to safely pass juvenile salmon through hydroelectric dams in the Pacific Northwest has been underway for over thirty-five years. In the 1970s and early 1980s, researchers showed that sluiceways at Bonneville, Ice Harbor, and The Dalles dams passed a relatively high proportion of smolts in a relatively low proportion of the flow (Willis and Uremovich 1981; Johnson et al. 1982; Nichols and Ransom 1981, respectively). Sluiceway operations for juvenile fish passage have been employed at some dams ever since to aid juvenile fish passage. In

1995, a major Corps program to develop surface flow outlets was initiated. Work in 1995 and subsequent years included prototypes at Bonneville, Ice Harbor, John Day, Lower Granite, and The Dalles dams. Surface flow outlet research has been summarized by Johnson et al. (1997), Dauble et al. (1999), and Sweeney et al. (2007) for the region as a whole; by Johnson and Giorgi (1999) and Johnson and Carlson (2001) for Bonneville Dam; and, by Johnson et al. (2005a) for Lower Granite Dam. A common concern expressed in these reviews was that, despite many years of research, information was lacking on the relationship between fish behavior and flow-field features, especially in the zone within about 10-20 m of SFO entrances.

Surface flow outlets are intended to create a flow field in the forebay that juvenile salmon can discover and utilize to move downstream. Although they generally follow the bulk flow downstream through reservoirs, fish sometimes meander when they encounter slow water in the forebays of dams (Adams et al. 1998). Assuming smolts discover the SFO flow net, a key point is whether they will react positively or negatively, i.e., will they enter or avoid the entrance? Discovery of a SFO flow net is only part of the issue; another part is for fish to actually follow the flow field and pass into the entrance. Efforts to improve SFO passage led to the spillway weir concepts, but there may be other, less expensive approaches such as the temporary spillway weir at McNary Dam. To develop these approaches, basic empirical data on fish response to SFO flow fields is needed to help coalesce engineering design guidelines.

Many previous studies have investigated fish/flow relationships as they relate to SFO development (Table 1.1). The following examples show limitations of previous research approaches. To investigate "why the Wells Dam SFO works so well", Johnson (1996) collected simultaneous mobile hydroacoustic and ADCP data in the dam forebay in 1995. There was no relationship between smolt density and water velocity. In fact, the variable most useful for explaining variation in smolt density was water depth. Variability in the fish density data was much greater than variability in the water data. Hedgepeth et al. (2002) used a sonar tracker based on principles of tracking radars to collect three-dimensional smolt movement data at The Dalles Dam sluiceway. They calculated movement probabilities using a Markov chain analysis and correlated the movement probabilities with hydraulic data from a computational fluid dynamics (CFD) model (e.g., Rakowski et al. 2006). No significant correlations were detected between the behavioral and hydraulic variables. The researchers thought there was a problem with temporal and spatial synchrony between the fish and water data sets. By synchrony we mean a match in space and time between fish and water data. At the Bonneville Dam Second Powerhouse corner collector SFO, a research team used a Dual Frequency Identification Sonar (DIDSON) to quantify fish movements (Ploskey et al. 2005). This was the beginning of an effort to survey multiple SFOs to elucidate patterns in fish behavior that developers might use to design SFOs. Water velocity data from a CFD were superimposed on the DIDSON fish data analyzed for Markov passage probabilities. While informative, the authors did not analytically merge fish and flow because it was cost prohibitive to do the large number of steady-state CFD runs necessary to cover the broad range of flow conditions over which they had fish data. Again, there was an issue of synchrony between the fish and water data sets.

Table 1.1. Research on Fish Movements and Flow Fields in the Anadromous Fish Evaluation Program.

Year(s)	Project	Fish Data	Water Data	Technical Approach	Findings	Citation
1995	Wells	Mobile hydroacoustics	ADCP	Multivariate & geostatistical analysis	No association between smolt density and water velocity. Depth was the most important independent variable.	Johnson (1996)
1995	The Dalles	Split hydroacoustics	Physical scale model 1:25	Vector analysis	Difficult to synchronize fish and water data. Presented a method for fish swimming effort vector.	Johnson, R.L. et al. (1995; 1998)
1997-1998	Snake R.	Radio telemetry	CFD	FINS model	2D, broad-scale, individual-based particle tracking model had reasonable correlations with observed travel times; not empirical	Scheibe and Richmond (2002)
1998-2000	Lower Granite, Bonn. 1	Multi-beam hydroacoustics	CFD	Vector analysis	Difficult to synchronize fish and water data. Short fish tracks were difficult to analyze.	Johnson, R.L. et al. (2001)
2000	Bonn. 1	Split hydroacoustics	ADCP	Vector analysis	Good synchrony, although sample volume was small; did not analyze further than vectors	Johnson, R.L. et al. (2001)
2000	The Dalles	Sonar tracker hydroacoustics	CFD	Correlation analysis using Markov data	Reasonably good fish/water synchrony, but variability in fish movement was high, leading to minimal or no correlation between Markov transition probabilities and hydraulic variables.	Hedgepeth et al. (2002)
2004	The Dalles	DIDSON+2 axis rotator	CFD	Multivariate analysis	Some significant variables explaining fish displacement, but synchrony poor	Scheibe et al. (unpubl.)
2004	The Dalles	DIDSON+2 axis rotator	CFD	Artificial neural network	Analysis pending	Hedgepeth et al. (unpubl.)
2005	Bonn. 1 and 2	DIDSON+2 axis rotator	CFD	Visualization	Informative to superimpose fish and water data, but not quantitative.	Ploskey et al. (2005)
1998-2005	Lower Granite, Rocky Reach, Wanapum	Acoustic telemetry	CFD	NFS model	three-dimensional, fine-scale, individual-based particle tracking model using fish behavior algorithms coupled with concurrent flow data; synchrony difficult	Goodwin et al. (2006)

In contrast to the empirical studies at Wells, The Dalles, and Bonneville dams, Goodwin et al. (2006) have worked since about 1998, much of the time at Lower Granite Dam (LGR), to develop a model that predicts three-dimensional fish movements in response to hydrodynamic data from a CFD. This model is called the Numerical Fish Surrogate (NFS). Movement rules and behavior coefficients are systematically adjusted during "calibration" until virtual fish movements approximate observed fish data from the field. Successful implementation of the NFS, thus, depends on fish movement data from field studies and should benefit from data herein on fish/flow relationships.

1.2 Objectives

This study provides information on juvenile salmonid behaviors at McNary and The Dalles dams that can be used by the USACE, fisheries resource managers, and others to support decisions on long-term measures to enhance fish passage. We collected data during April 21-26, 2007 at McNary Dam and May 1 to July 12, 2007 at The Dalles Dam. The research objectives were as follows.

McNary Dam -- Conduct a pilot study of simultaneous fish behavior and water velocity data in the nearfield (< 20 m) of a prototype Temporary Spillway Weir (TSW) to:

1. Establish the deployment procedure and collect preliminary data.
2. Assess the feasibility of this technique to study smolt responses to hydrodynamics at a McNary TSW (No. 2).

The Dalles Dam -- Apply new empirical data from simultaneous remote sensing techniques and computational fluid dynamics modeling in the nearfield of the sluiceway to:

1. Characterize fish behavior and water velocity patterns.
2. Examine descriptive and statistical associations between juvenile salmonid movements and hydrodynamic conditions immediately upstream of the SFO entrances.
3. Address guidelines for hydraulic parameters of the flow net upstream of this SFO that would be conducive to juvenile salmonids passing into the SFO entrance.

1.3 Report Content

This report has five sections and one appendix. Following the introduction in Section 1, the methods are described in Section 2. Section 3 contains the results. Section 4 contains discussion, including conclusions and recommendations. Section 5 lists the literature we cited. Appendix A has the methods for data processing and analysis.

2.0 Methods

This section includes the general approach, data collection, data processing, and analysis. We obtained hydraulic data from *in situ* measurements of water velocity using an acoustic Doppler current profiler (ADCP) and from a computational fluid dynamics (CFD) model. We collected fish behavior data using an acoustic imaging camera. We processed and analyzed the data using custom manual tracking software and Matlab, C++, and SAS code.

2.1 General Approach

To achieve temporal and spatial synchrony between the physical and biological measurements to study relationships between fish and flow, we collected and merged simultaneous DIDSON (fish) and ADCP (water) data. The DIDSON and ADCP were mounted together (Figure 2.1) on a pole connected to a single axis rotator. The ADCP and DIDSON acoustic beams sampled similar water volumes; note, the sample volume (0.25 m range bins) increased in size as distance from the transducers increased (Figures 2.2 and 2.3). This study was the first time such data sets were merged and analyzed, alleviating the issue of temporal synchrony mentioned earlier.

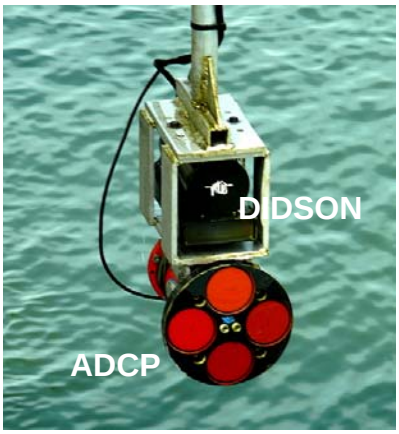

Figure 2.1. ADCP/DIDSON.

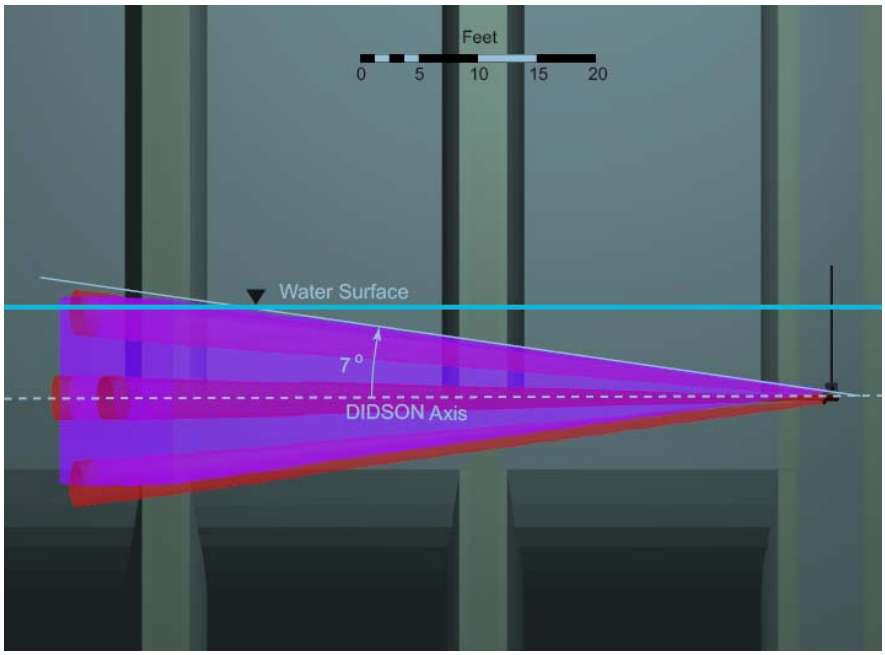

Figure 2.2. Sample Volume -- Side View of Simultaneous ADCP (red) and DIDSON (purple) Acoustic Beams. The background is The Dalles Dam powerhouse. In this schematic, the DIDSON was aimed across the face of the dam in a northeast direction.

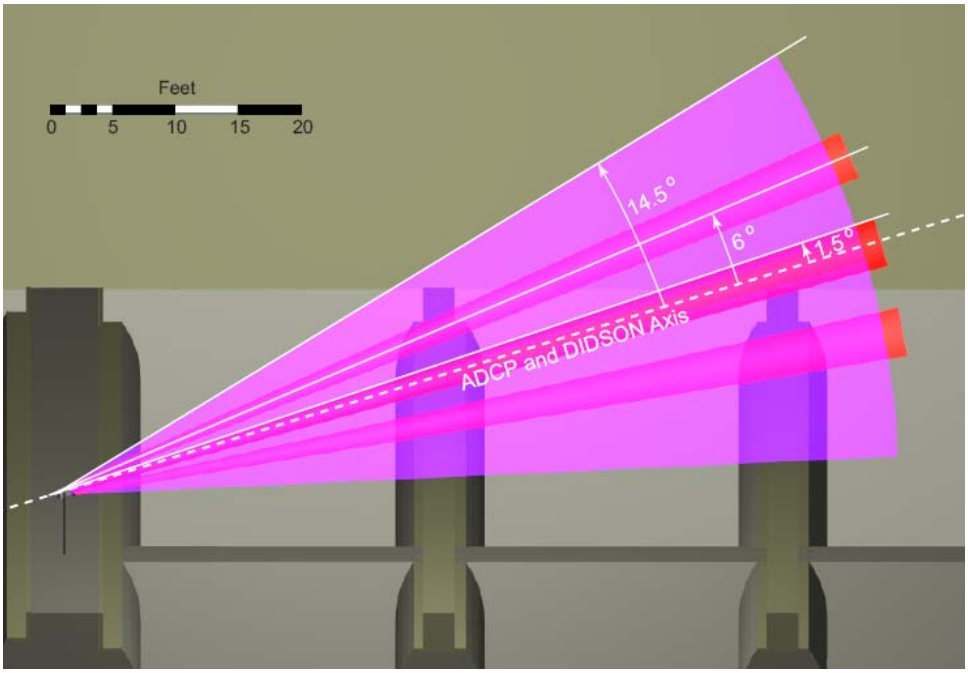

Figure 2.3. Sample Volume -- Plan View of Simultaneous ADCP (red) and DIDSON (purple) Acoustic Beams. The background is The Dalles Dam powerhouse. The projection of the sloping piers into the beams is an artifact of the graphic.

The main drawback of this approach, however, is that the size of the ADCP sample volume can be large relative to the size of the fish, depending on range from the instrument. Therefore, we supplemented the study with CFD modeling for scenarios when dam operations in the vicinity of the DIDSON were relatively constant. The CFD allowed fine-scale spatial resolution, but was steady-state temporally. The ADCP revealed the temporal variation in water velocity, but at ranges greater than about 6 m had low spatial resolution (1 m wide). The two techniques were complementary.

2.2 Field Data Collection

2.2.1 ADCP

Use of acoustic Doppler current profilers to collect water velocity profiles and river discharge has been widely documented in the technical literature since the 1980s (see Gordon 1989; Schott 1987). In this study, the ADCP (Workhorse Teledyne RD Instruments, Inc. [RDI]) was not boat-mounted, but instead placed on a movable mount connected to the dam itself (Figures 2.2 and 2.3). Prior applications on the Columbia River system where ADCPs were mounted to the dam structure include measurements at turbine intakes and spillway gates (Johnson et al. 2005b) and near the exits of draft tubes (Cook et al. 2007).

ADCPs work by transmitting acoustic pulses (at 600 kHz for this project) from each of four diverging acoustic transducers (see Figure 2.4). This transducer arrangement is known as a Janus configuration. The custom-built narrow foot-print ADCP had transducers spaced at 90-degree azimuth intervals from one another and with a vertical angle of 6-degrees (Figure A.2 in Appendix A) as compared to the standard 20-degree angle. After the pulse is emitted, the ADCP then receives and

processes returned echoes from points at successively greater distances along the beams to determine how much the frequency has changed. The difference in frequency between transmitted and reflected sound is proportional to the relative velocity between the ADCP and the scatters in the water based on the Doppler shift. The profiling range over which an ADCP can resolve water velocities depends upon the frequency of the acoustic signal. Generally, the lower the frequency the farther the ADCP can measure through the water column however the greater the Doppler uncertainty, all other settings being equal. For example, the typical profiling range of the 600-kHz model used in this study is approximately 20 m (65 ft). The single ping Doppler uncertainty for the 600-kHz is 5.7 cm/s (1 m bin size, default settings).

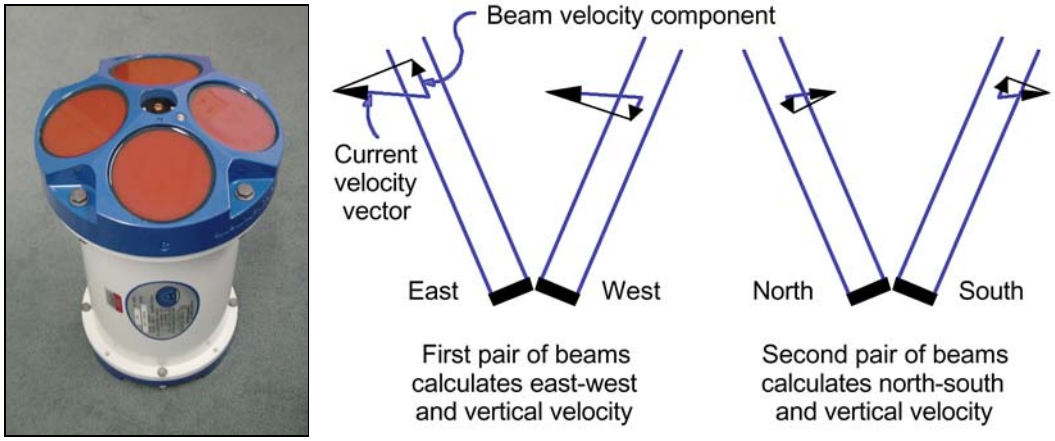

Figure 2.4. Photograph of a 600-kHz ADCP (left) and Beam Velocity Schematic (right, after RDI 1996). Cardinal directions given in the right-side figure are for descriptive purposes only, and deployment orientation of the ADCP beams was not specific to any coordinate system.

Properties of each beam, including signal correlation magnitude and echo intensity with distance from the transducers, are output from the device. Signal correlation magnitude data show the magnitude of the echo autocorrelation at the lag used for estimating the Doppler phase change. The ADCP represents this magnitude by a linear scale between 0 and 255, where 255 is a perfect correlation (i.e., a solid target). Echo intensity refers to the returned signal strength which is useful for determining cross-talk if a beam hits a solid object and for range measurement to a solid object (e.g., fish body, bottom or structure).

Each ADCP measurement consists of four one-dimensional water velocity profile measurements along the axis of each acoustic beam (see Figure 2.4). These one-dimensional beam velocities sample only a small volume of water because the acoustic beam emitted by each transducer is intentionally focused and narrow. Under the assumption that water currents are nearly-uniform in the plane perpendicular to the transducers' mutual axis, the four one-dimensional beam profile measurements can be combined to compute a profile of three-dimensional water velocities (RDI 1998a). Because only three beams are necessary to compute a three-dimensional water velocity with a Janus-configured ADCP, the fourth beam velocity measurement is used for redundancy and to check that the velocity field is sufficiently homogenous. It should be noted that even if the uniformity

assumption is not strictly met for resolving a three-dimensional velocity vector, the profiles of velocity magnitude collected along the axis of each beam are still valid measurements.

The ADCP operation scripts were configured to sample data at a frequency of 1 Hz. The profile range was 20-m and was divided into individual 0.25-m cells (80 cells total). At McNary data were collected at the single orientation for about 8 days. The instruments were rotated through four beam orientations at The Dalles Dam and were data collected at a position for 24-hours during each 4-day sampling period. Procedures outlined by RDI were used to check internal electronic components and the transducer/receiver (RDI 1998b). The ADCP passed all checks.

2.2.2 DIDSON

To assess fish movements in the nearfield (< 20 m) in front of the sluiceway, an acoustic imaging device, the DIDSON, was deployed. The DIDSON bridges the gap between conventional scientific fisheries sonar, which can detect acoustic targets at long ranges but cannot record the shapes of targets, and optical systems, which can record images of fish but are limited at low light levels or when turbidity is high. The DIDSON has a high resolution and fast frame rate enabling it to substitute for optical systems in turbid or dark water. This device, for example, was successfully applied at The Dalles Dam in previous research on predator distributions relative to the J-occlusion plates (Johnson et al. 2003), and during a similar study to determine sluiceway entrainment zones at TDA in 2004 (Johnson et al. 2005b). Figure 2.5 shows an image of smolts observed using the DIDSON.

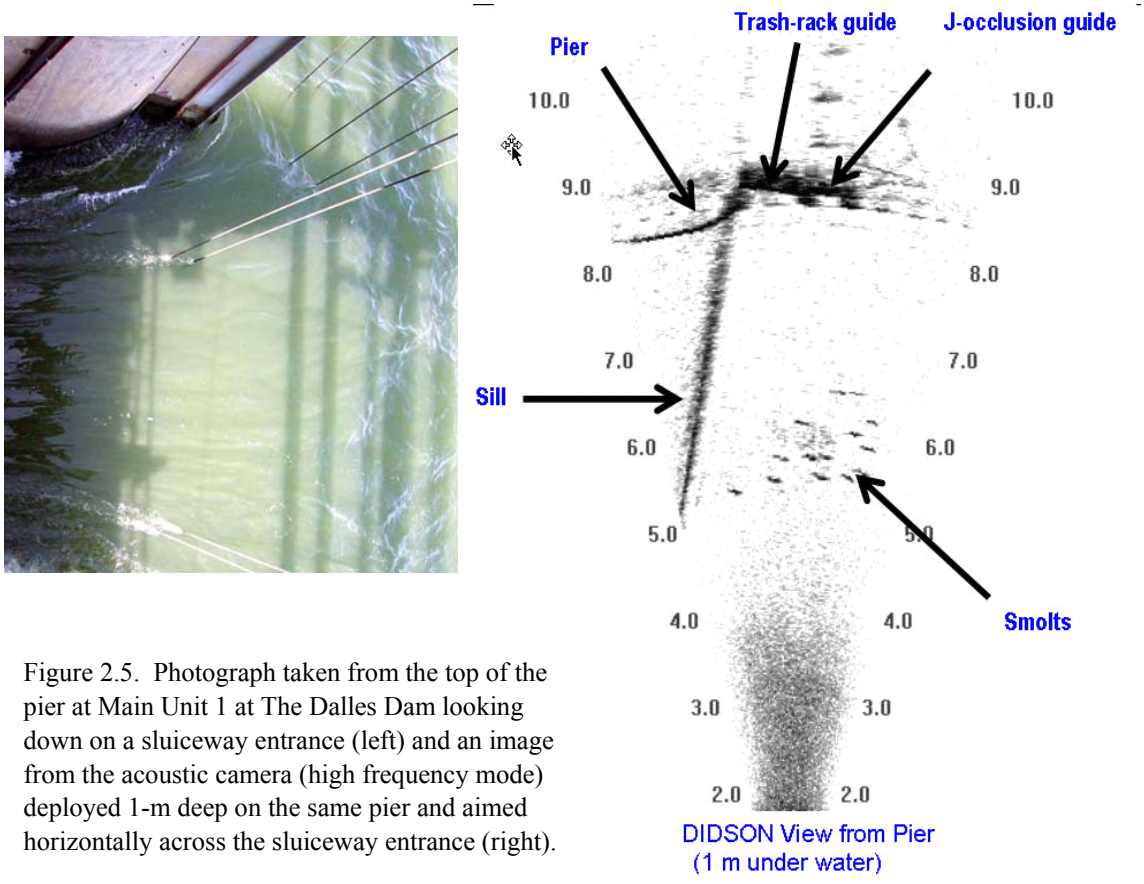

Figure 2.5. Photograph taken from the top of the pier at Main Unit 1 at The Dalles Dam looking down on a sluiceway entrance (left) and an image from the acoustic camera (high frequency mode) deployed 1-m deep on the same pier and aimed horizontally across the sluiceway entrance (right).

At both dams, the DIDSON frequency was set at 1 MHz ("low" frequency) to maximize the range (18 m) for data collection. During July at The Dalles Dam, however, we used the high frequency (1.2 MHz) to increase resolution at the sluiceway at the expense of range (11 m). At 1 MHz, the DIDSON has 48 individual beams 0.6 deg by 14 deg. The resulting sample volume was 29 deg wide by 14 deg high. The ping rate was 7 frames per sec. Belcher et al. (1999) describe the basic operational characteristics and specifications of the DIDSON acoustic camera.

2.2.3 Sampling Locations and Orientations

At McNary Dam on April 11, 2007, the DIDSON and ADCP were deployed at Elevation 333 ft (reference means sea level; MSL) on a rail on the pier between Bays 19 and 20 and aimed horizontally upstream and approximately 30 deg towards the south off the face of the dam to sample in the nearfield of TSW 2 at Bay 19 (Figures 2.5 and 2.6).

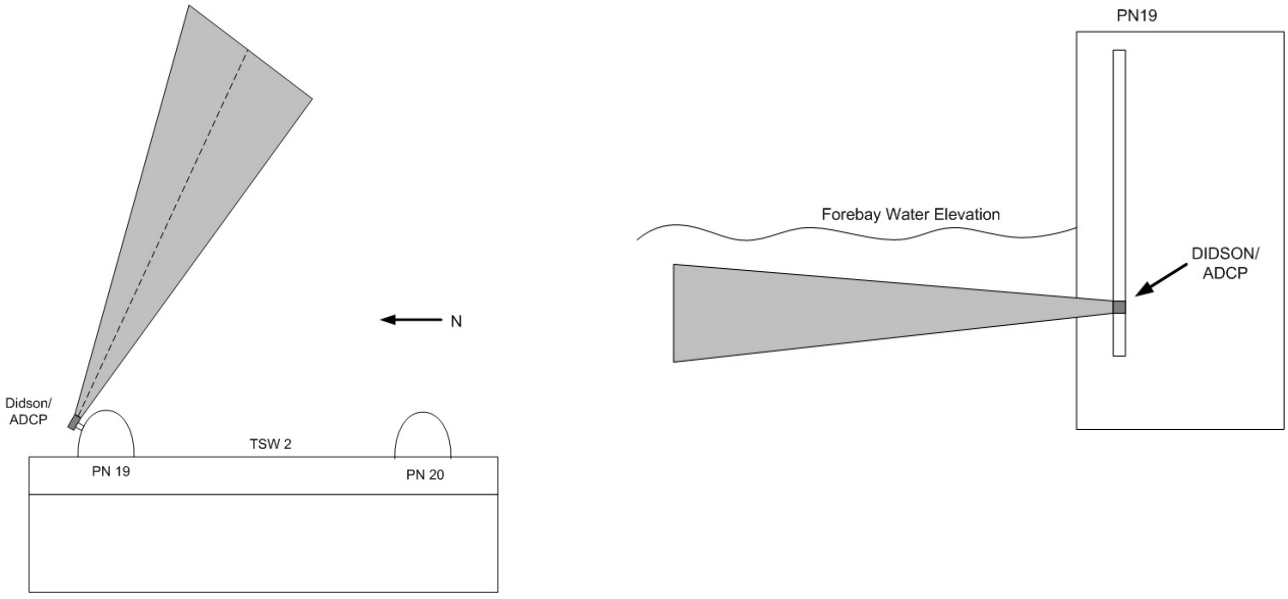

Figure 2.5. Plan (left) and Side (right) Views Showing ADCP and DIDSON Instrument Location and Sample Volumes Relative to TSW 2 at McNary Dam, 2007

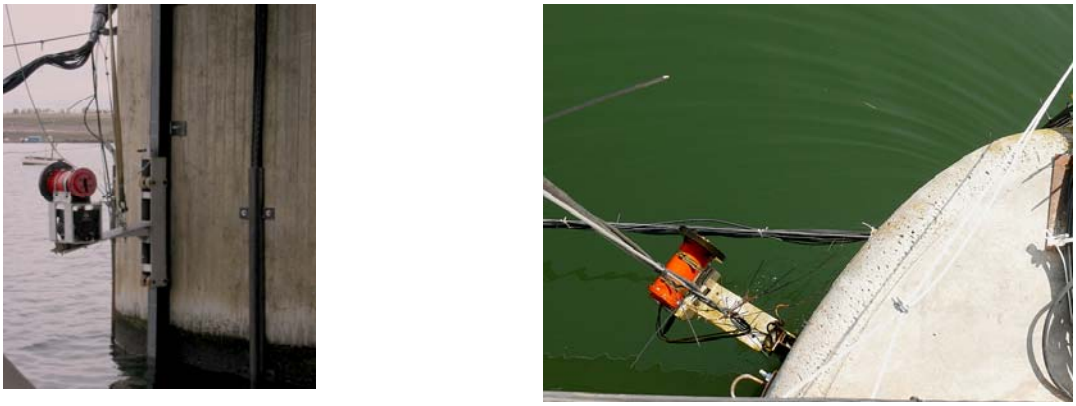

Figure 2.6. Photographs of ADCP/DIDSON Deployment at McNary Dam, 2007

At The Dalles Dam, the DIDSON and ADCP were mounted on a single axis rotator and deployed at Elevation 152 ft MSL on a rail on the pier between Fish Unit 2 and Main Unit 1 (Figures 2.7 and 2.7). The instruments were aimed horizontally upstream off the face of the dam to sample in the nearfield of Sluice 1-1 and 1-2. We manually rotated the apparatus once per day in a random sample sequence to cover the four aiming angles (Figure 2.7) which had a 5 deg overlap.

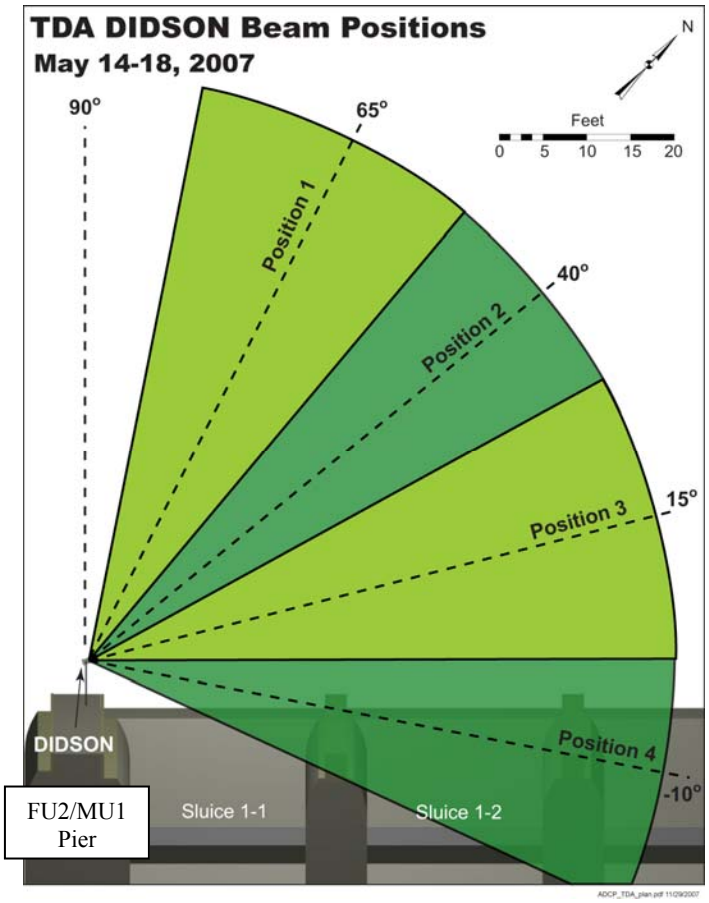

Figure 2.7. Plan View Showing ADCP and DIDSON Instrument Location and Sample Volumes Relative to the Sluiceway at The Dalles Dam, 2007

Figure 2.8. Photograph of the ADCP/DIDSON at The Dalles Dam, 2007

2.2.4 Sampling Schedule and Environmental Conditions

At McNary Dam, sampling occurred 24 h/d at the beginning of the spring outmigration from April 20 to April 26, 2007 (Figure 2.9). Total discharge during sampling was about 220 kcfs with about 90 kcfs spill (Figure 2.10). The equipment was retrieved on April 27, 2007 and transported to The Dalles Dam for similar research. This sampling period was necessary because of several factors. Since the contract was awarded after the fish spill season had begun, a spillway closure was required to deploy the gear. Fortunately, this occurred for the purpose of another study on April 11. Because more closures would diminish fish protection measures at the dam, we sampled consecutive days for the six days called for in the contract. We retrieved the equipment using a crane and hook apparatus without closing the spill gates.

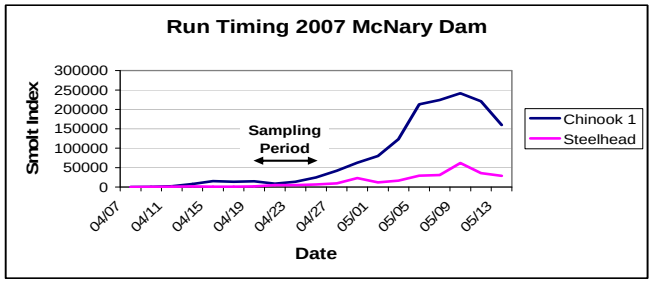

Figure 2.9. Run Timing at McNary Dam, 2007. Data are from Data Access in RealTime (DART) (http://www.cbr.washington.edu/dart/).

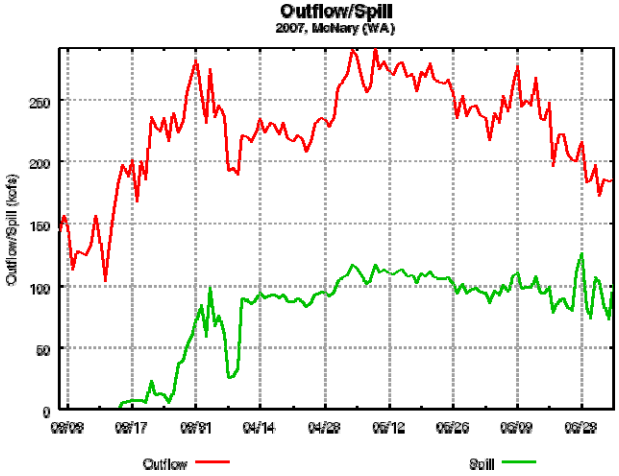

Figure 2.10. Total River Discharge (1,000 cubic feet per second; kcfs) and Spill Discharge (kcfs) at McNary Dam, Spring 2007. This figure was obtained from DART.

At The Dalles Dam, we sampled 24 h/d during three four-day periods in both spring and summer according to the schedule in Table 2.1. These sampling episodes included the downstream migrations of yearling and subyearling fish in spring and summer, respectively (Figure 2.11). River discharge ranged from about 150 to 280 kcfs during the ADCP/DIDSON sampling (Figure 2.12). Voluntary spill for fish protection commenced on April 10 at 40% of total project discharge.

Table 2.1. Schedule for ADCP/DIDSON Sampling at the Sluiceway at The Dalles Dam. Positions (aiming angles) are shown in Figure 2.7.

Season	Period	Position 1	Position 2	Position 3	Position 4
Spring	Early	5/3/2007	5/4/2007	5/1/2007	5/2/2007
	Middle	5/17/2007	5/14/2007	5/15/2007	5/16/2007
	Late	5/21/2007	5/23/2007	5/26/2007	5/22/2007
Summer	Early	6/14/2007	6/13/2007	6/12/2007	6/11/2007
	Middle	6/26/2007	6/25/2007	6/24/2007	6/27/2007
	Late	7/9/2007	7/10/2007	7/11/2007	7/12/2007

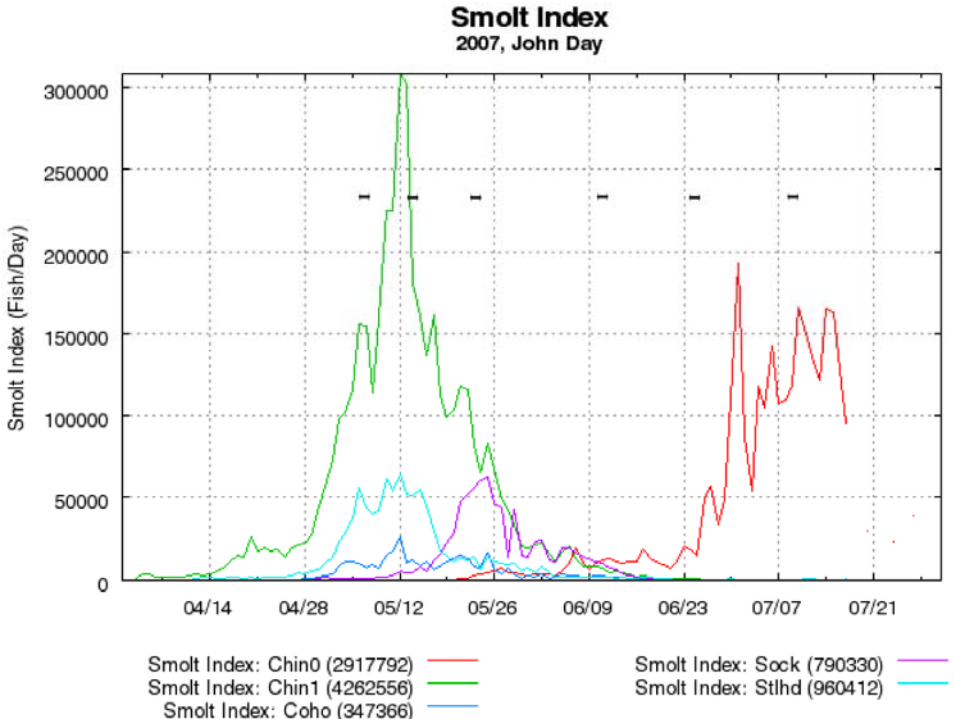

Figure 2.11. Run Timing at John Day Dam, 2007. Data are from DART.

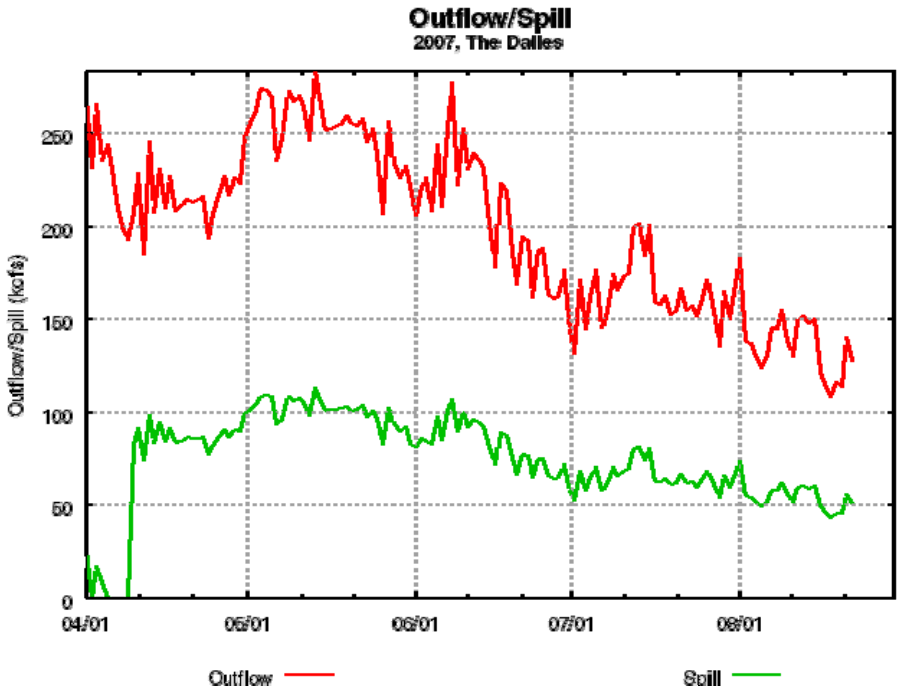

Figure 2.12. Total River (Outflow) and Spill Discharge (kcfs) during Spring and Summer 2007 at The Dalles Dam. The figure was obtained from DART.

2.3 Computational Fluid Dynamics Modeling

A computational fluid dynamics (CFD) model of The Dalles Dam forebay was used to simulate the hydraulic conditions for various operational scenarios. All simulations used STAR-CD version 4.02, a commercial CFD solver (CD-Adapco 2007). The computational meshes used for these simulations were created using the Gridgen software package (www.pointwise.com) and was based on bathymetry). Additional details on the TDA CFD model configuration and confirmation using field data measurements are available in Rakowski et al. (2006).

A new element added to the CFD model in this study was the inclusion of the The Dalles Dam ice and trash sluiceway flows. The previous TDA forebay model (Rakowski et al. 2006) approximated the water surface using a conventional horizontal rigid-lid at a fixed forebay elevation. As water enters the sluiceway, however, the water surface is drawn down. To better represent the water acceleration associated with the surface drawdown it was necessary to modify the rigid-lid boundary to approximate the water surface shape. A free-surface simulation of a limited forebay zone including the sluiceway was performed and the non-uniform water surface shape extracted for use in constructing a new rigid-lid mesh. The complete CFD model then included the entire forebay, sluiceway entrance, and sluiceway channel. Although field measurements of the sluiceway discharge were not available, the simulated discharge through each entrance of the sluiceway at Main Unit 1 were compared to estimated values computed by Portland District Hydraulic Design (Steve Schlenker, personal communication) using weir-formulas and ranged from 1% to 12% of the calculated values.

Steady-state boundary conditions for the CFD model were applied to a scenario that approximated the actual project operations that occurred during the spring and summer 2007 conditions time periods used in the DIDSON data processing (Table 2.2). Simulation results were saved for later extraction and analysis with the DIDSON data.

Table 2.2. Scenario for CFD Modeling of The Dalles Dam Forebay, 2007. Forebay elevation was set at 158.5 ft. Discharge (Q) is in thousand cubic feet per second (kcfs).

	Scenario 1
Powerhouse Q	163.0
Sluiceway Q	4.5
MU 1	9.9
MU 2	9.8
Spillway Q	110.0
Total River Q	273.0

In addition to the CFD model for The Dalles Dam forebay, a single bay model of a temporary spillway weir at McNary dam was also simulated. The purpose of this model was to provide a general picture of the approach flow to compare with that at The Dalles Dam. The McNary TSW model used a forebay elevation boundary condition of 340 feet.

2.4 Data Processing and Analysis

This section contains information on the subsample data set and the analysis variables. Additional data processing and analysis methods are explained in Appendix A.

2.4.1 Subsample Data Set

The DIDSON acoustic imaging device and the ADCP data sets were large (4 and 529 GB, respectively). Each 20-minute raw DIDSON file was 203 MB and a 24-hour ADCP file amounted to 150 MB. To process the data in a timely manner and process enough data to have a meaningful data set, it was necessary to subsample the data (Table 2.3). The subsample priorities were data from each a) block, except Block 4 when few fish were present; b) aiming position; and c) diel/crepuscular period, i.e., dawn, day, dusk, and night.

Table 2.2. Hours Processed for the 2007 Data Set. Asterisk (*) indicates only 20 min of data were processed due to large number of fish.

Spring						Summer					
Block 1		Block 2		Block 3		Block 4		Block 5		Block 6	
Date	Hour	Date	Hour	Date	Hour	Date	Hour	Date	Hour	Date	Hour
1-May	1900*	14-May	1900	none		11-Jun	1900	24-Jun	1800	1-Jul	1900
	2300*		2300				2300		2100		2300
2-May	0600*	15-May	0200			12-Jun	0600	25-Jun	0000	2-Jul	0600
	1300*		0600				1200		0300		1300
	1900*		1000				1900		0600		1900
	2300*		1300				2300		0900		2300
3-May	0600*		1600			13-Jun	0600		1200	3-Jul	0600
	1300*		1900*				1200		1500		1300
	1900*		2300*				1900		1800		1900
	2300*	16-May	0200				2300		2100		2300
4-May	0600*		0600*			14-Jun	600	26-Jun	0000	4-Jul	0600
	1300*		1000				1300		0300		1300
	1900*		1300*				1900		0600		1900
	2300*		1600*				2300		0900		2300
5-May	0600*		1900*			15-Jun	0600		1200	5-Jul	0600
	1300*		2300*				1300		1500		1300
		17-May	0200						1800		
			0600*						2100		
			1000					27-Jun	0000		
			1300*						0300		
			1600						0600		
			1900*						0900		
			2300*						1200		
		18-May	0200						1500		
			0600*						1800		
			1000						2100		
			1300*					28-Jun	0000		
			1600						0300		
									0600		
									0900		
									1200		
									1400		

2.4.2 Variables

The coordinate system relative to the dam was as follows:

- X-dimension is parallel to the face of the dam; positive X is toward the east;
- Y-dimension is perpendicular to the dam; positive Y is toward the forebay;
- Z-dimension is vertical; positive Z is upward.

The following categorical variables were used as independent variables in the analysis.

- Dam – McNary or The Dalles
- Season – spring (April-May) and summer (June-July)
- Daycode – dawn (1), day (2), dusk (3), and night (4)> The times of twilight, sunrise and sunset were taken from tables published by the US Naval Observatory for The Dalles and for Umatilla Oregon (http://aa.usno.navy.mil/data/docs/RS_OneYear.php). Twilight period definitions were modified (extended) by 30 minutes before and after.
- Distance from SFO – near is < 3 m in the y-dimension and far is greater than or equal to 3 m, as determined by the 50% break in the number of event observations
- School – no (1-2 fish) or yes (>2 fish)

The following hydraulic variables were also used as independent variables in the analysis.

- Water Speed for the X, Y, and Z dimensions = U_W, V_W, W_W
- Water Speed (m/s) $R = \left(U_W^2 + V_W^2 + W_W^2\right)^{0.5}$
- Temporal Acceleration Index (m/s^2) = $\left[\left(\frac{\partial U}{\partial t}\right)^2 + \left(\frac{\partial V}{\partial t}\right)^2 + \left(\frac{\partial W}{\partial t}\right)^2\right]^{0.5}$
- Total Acceleration for the X, Y, and Z dimensions

$$A_x = \frac{DU}{Dt} = \frac{\partial U}{\partial t} + U\left(\frac{\partial U}{\partial x}\right) + V\left(\frac{\partial U}{\partial y}\right) + W\left(\frac{\partial U}{\partial z}\right)$$

$$A_y = \frac{DV}{Dt} = \frac{\partial V}{\partial t} + U\left(\frac{\partial V}{\partial x}\right) + V\left(\frac{\partial V}{\partial y}\right) + W\left(\frac{\partial V}{\partial z}\right)$$

$$A_z = \frac{DW}{Dt} = \frac{\partial W}{\partial t} + U\left(\frac{\partial W}{\partial x}\right) + V\left(\frac{\partial W}{\partial y}\right) + W\left(\frac{\partial W}{\partial z}\right)$$

where, (*U, V, W*) are the velocity components in the dam coordinate system. *DU/Dt*, etc are called the material derivatives that relate the Lagrangian rate of change for a fluid parcel to the Eulerian derivatives. $\partial U/\partial x$, are the velocity gradients which compose the strain rate tensor. The time derivative part of the

acceleration is called the local acceleration. The part with spatial derivatives is called the convective acceleration.

- Total Acceleration =

$$\left(A_x^2 + A_y^2 + A_z^2\right)^{0.5}$$

- Total Strain Index[1] (s^{-1}) =

$$\left|\frac{\partial U}{\partial x}\right| + \left|\frac{\partial V}{\partial x}\right| + \left|\frac{\partial W}{\partial x}\right| + \left|\frac{\partial U}{\partial y}\right| + \left|\frac{\partial V}{\partial y}\right| + \left|\frac{\partial W}{\partial y}\right| + \left|\frac{\partial U}{\partial z}\right| + \left|\frac{\partial V}{\partial z}\right| + \left|\frac{\partial W}{\partial z}\right|$$

The following fish response variables were computed at the event-level from the following ping to ping data and used as dependent variables in the analysis. Units are m/s.

- Fish Speed $FS = \left(FV_x^2 + FV_y^2\right)^{0.5}$, where FV_x is the X-component of fish velocity and FV_y is the Y-component (see equations on next page).

- Fish Speed (intermediate pings) = $\dfrac{\left[\left(x_{i+1} - x_{i-1}\right)^2 + \left(y_{i+1} - y_{i-1}\right)^2\right]^{0.5}}{\left(t_{i+1} - t_{i-1}\right)}$

- Fish Speed (last ping) = $\dfrac{\left[\left(x_n - x_{n-1}\right)^2 + \left(y_n - y_{n-1}\right)^2\right]^{0.5}}{\left(t_n - t_{n-1}\right)}$

- Fish Speed (event average of ping-ping estimates) =

$$\frac{1}{n}\left(\frac{\sqrt{\left(x_2 - x_1\right)^2 + \left(y_2 - y_1\right)^2}}{\left(t_2 - t_1\right)} + \sum_{i=2}^{n-1}\frac{\sqrt{\left(x_{i+1} - x_{i-1}\right)^2 + \left(y_{i+1} - y_{i-1}\right)^2}}{\left(t_{i+1} - t_{i-1}\right)} + \frac{\sqrt{\left(x_n - x_{n-1}\right)^2 + \left(y_n - y_{n-1}\right)^2}}{\left(t_n - t_{n-1}\right)}\right)$$

- Fish Velocity X dimension (U_F) =

For endpoints $\dfrac{x_{i+1} - x_i}{t_{i+1} - t_i}$ or $\dfrac{x_{i+2} - x_{i-1}}{t_{i+2} - t_{i-1}}$ central difference for interior pings

- Fish Velocity Y dimension (V_F) =

For endpoints $\dfrac{y_{i+1} - y_i}{t_{i+1} - t_i}$ or $\dfrac{y_{i+2} - y_{i-1}}{t_{i+2} - t_{i-1}}$ central difference for interior pings

- Fish Swimming Effort X dimension (Xeffort) $U_E = U_F - U_w$

[1] This is the same as the spatial velocity gradient tensor used by Goodwin et al. (2006) to represent total hydraulic strain.

- Fish Swimming Effort Y dimension (Yeffort) $V_E = V_F - V_w$
- Fish Swimming Effort (Effort Speed)

$$E = \left(U_E^2 + V_E^2\right)^{0.5}.$$

We analyzed the time series of whether a fish event was swimming with the flow or not. This could be a useful measure for associating with directed or rejection behavior. Calculation of whether a fish is swimming "with the flow" or "against it" uses fish effort (U_E, V_E) and water velocity (U_W, V_W). If the angle θ between the effort vector and the water vector is less than 90 degrees, fish are swimming "with the flow". To calculate the angle, construct a triangle where the effort and water speed vectors are two sides, with magnitudes E and W. The third side has magnitude

$$M = \sqrt{\left(U_W - U_E\right)^2 + \left(V_W - V_E\right)^2}.$$

The law of cosines can be used to determine the angle θ, called the "swim angle", between water velocity (R) and swimming effort (E) vectors.

$$M^2 = E^2 + R^2 - 2ER\cos\theta,$$

Thus, fish swimming effort relative to water velocity, i.e., the projection of the swimming effort vector on the water velocity vector, called "effort-cos-theta", is as follows

$$E\cos\theta = \frac{E^2 + R^2 - M^2}{2R}.$$

2.4.3 Processing and Analysis Methods

The DIDSON data were processed manually to extract detailed information (see Section 2.4.2) about each observed fish or fish school. These data were analyzed by sorting and averaging to produce the information on "movement tallies." The ping-to-ping positional data from the manual tracking process were merged with water velocity and other hydraulic data extracted from the CFD for each particular X.Y position. From the merged data we then calculated fish-swimming-effort and effort-cos-theta (see Section 2.4.2). Standard Pearson correlations (Sokal and Rohlf 1981) were computed between the fish swimming data and the hydraulic data. Based on the results of the correlation analysis, non-linear regressions were applied to examine relationships between fish swimming and water velocity, accelerations, and strain. Processing and analysis methods are explained further in Appendix A.

3.0 Results

This section is organized into the following sequence of material: water velocity, fish observations, and fish behavior relative to hydrodynamics.

3.1 Water Velocity

Comparison of the ADCP and CFD results revealed an apparent problem with our application of the ADCP. The instrument was functioning properly, but the assumption that water velocities were sufficiently homogenous for a given range in the ADCP beams may not have been met, producing anomalous water velocity vectors. We plan to investigate this issue in collaboration with the instrument vendor. Pending resolution of this problem, all water-related and fish effort variables were calculated using the velocity fields simulated by the CFD model.

At McNary Dam, descriptive view of the approach velocity is shown in Figure 3.1. The general flow pattern shows approach paths inline with the spillbay. Velocities increase both in the horizontal and vertical planes from less than 1 m/s to over 5 m/s at the crest of the TSW. Within 5 m distance, velocities increase dramatically, especially near the pier nose and TSW crest.

At The Dalles Dam, flow approaches the sluiceway at Main Unit 1 in an oblique direction with velocity vectors that gradually turn into the entrance (Figure 3.2). Velocity magnitudes increase from less than 1 m/s in upstream of the piers to over 5 m/s as flow crosses the sluiceway sill into the discharge channel. This is similar to McNary, flow accelerates as it enters the sluiceway, but at TDA there is no free overfall and subsequent impact of water on the face of an ogee. Another key difference is that the slucieway entrances at TDA are located above the turbine intakes. Therefore, when turbine units are in operation a flow split occurs (Figure 3.2, elevation view).

The hydraulic variables described in Section 2.4.2 were extracted from the CFD simulation for an area approximately 20-m square that corresponded to the DIDSON sampling zone. Summary statistics for these hydraulic variables are listed in Table 3.1.

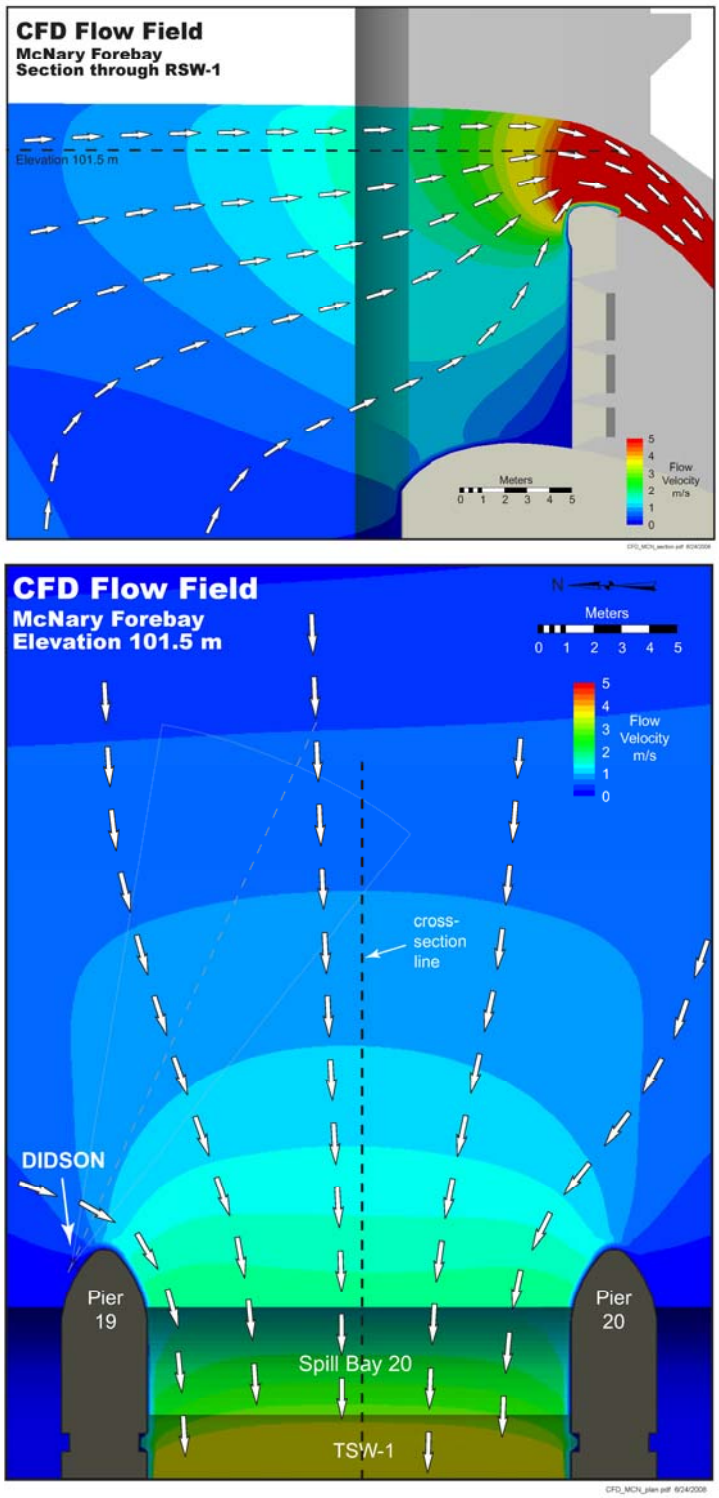

Figure 3.1. Sectional (top) and Plan (bottom) Views of the Simulated Velocity Field for a Single-bay CFD Model of the TSW at McNary Dam. Forebay elevation 340 ft MSL. TSW discharge 10.7 kcfs.

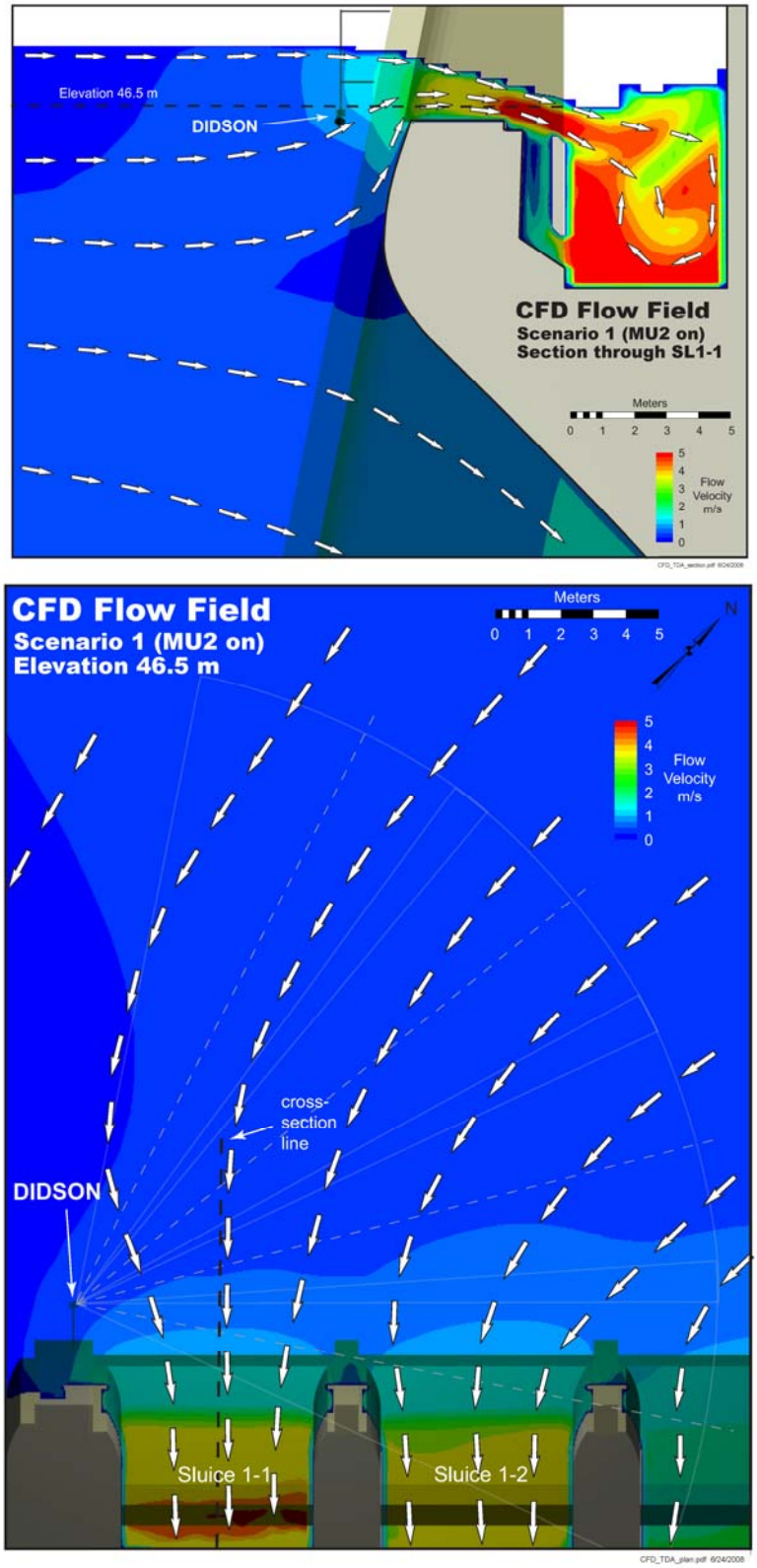

Figure 3.2. Sectional (top) and Plan (bottom) Views of the Simulated Velocity Field Near the Sluiceway Entrance SL 1-1 and SL 1-2 at Main Unit 1 at The Dalles Dam for Flow Scenario 1 (Table 2.2).

Table 3.1. Descriptive Statistics for Hydraulic Data from the CFD Model for Scenario 1 (Table 2.2).

Variable	Mean	Std Dev	Min	Max
U	-0.11	0.09	-0.78	0.32
V	-0.43	0.18	-2.15	-0.15
W	0.04	0.07	-0.01	0.53
VelocityMagnitude	0.46	0.18	0.25	2.23
dUdX	-0.03	0.03	-0.31	0.48
dVdX	0.00	0.04	-1.00	0.95
dWdX	0.00	0.01	-0.10	0.18
dUdY	0.00	0.03	-0.90	0.34
dVdY	0.06	0.09	-0.62	1.56
dWdY	-0.02	0.03	-0.30	0.53
dUdZ	0.04	0.02	-0.22	0.26
dVdZ	-0.01	0.05	-0.44	0.04
dWdZ	-0.03	0.06	-1.55	0.03
DXDT	-0.34	0.38	-8.33	4.42
DYDT	-0.15	0.34	-6.70	5.06
AU	0.00	0.02	-0.22	0.23
AV	-0.04	0.11	-3.52	0.09
AZ	0.01	0.02	-0.87	0.16
Acceleration	0.05	0.12	0.00	3.68
Strain	0.25	0.29	0.02	3.85

3.2 Fish Observations

Fish observation results include visualizations of fish and school tracks, movement tallies, and fish speeds.

3.2.1 Visualizations

The original data set for this study contained 3,691 events (observations of individual fish or schools of fish) (Table 3.2). The events were made up of 46,311 ping-to-ping observations (X coordinate, Y coordinate, time). Thus, on average, there were 13 ping-to-ping observations per event. However, after merging with the CFD data for Scenario 1, there were 22,878 ping-to-ping observations available for the fish/flow analyses.

The observation visualizations reveal the sample volumes and a mixture of individuals and fish schools at McNary (Figure 3.5A) and The Dalles (Figure 3.3B) dams. The sample volume at McNary Dam was limited to one aiming position because it was a feasibility study.

Table 3.2. Numbers of Observations Used in the Analyses

Dam	Season/Period	Number of Ping-to-Ping Observations
McNary	Spring/Day	4,675
	Spring/Night	3,899
The Dalles	Spring/Day	14,070
	Spring/Night	5,938
	Summer/Day	12,294
	Summer/Night	5,435
Total Fish Observations (fish only; before fish/flow merge)		46,311
Total Fish Behavior Relative to Hydrodynamics (after fish/flow merge Scenario 1; The Dalles only)		22,878

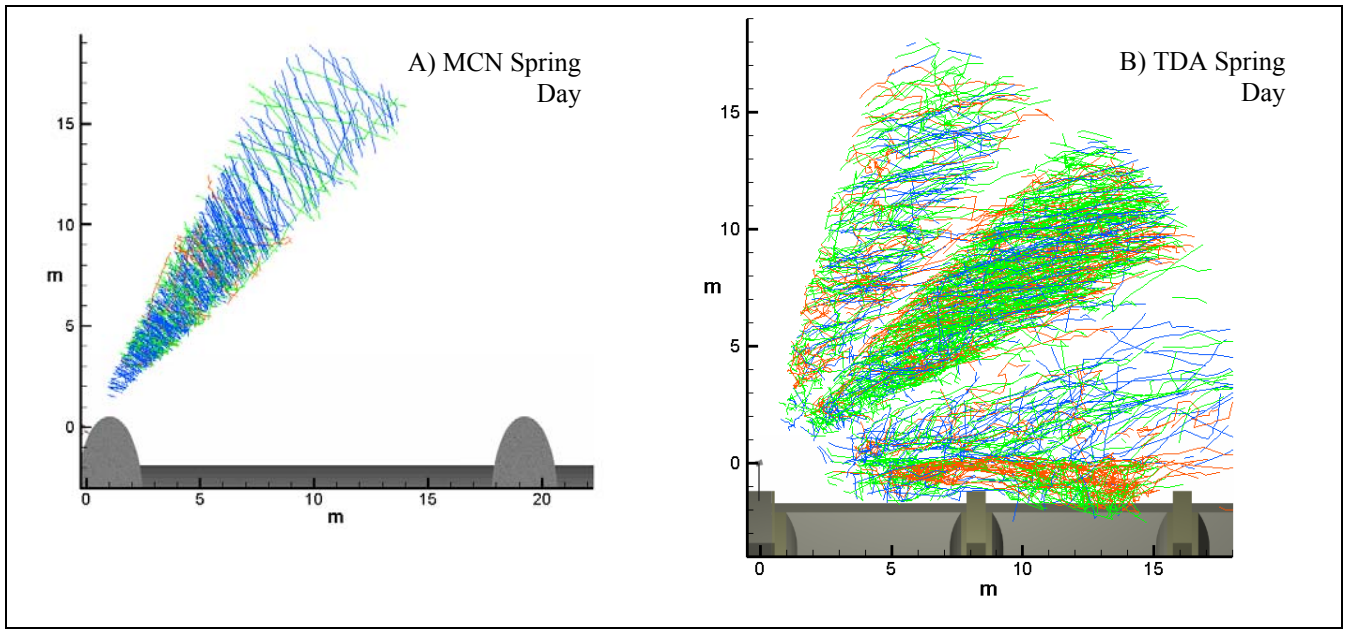

Figure 3.3. Plan View Visualization of Fish Events during Day, Spring 2007, McNary Dam (left) and The Dalles Dam (right). Blue = single fish; green = 3 to 10 fish; red >10 fish.

3.2.2 Movement Tallies

We characterized fish observations using the DIDSON data at surface flow outlets at McNary and The Dalles dams according to whether the events were schools (3 or more fish moving in unison) or individuals (1 or 2 fish), whether movement was directed (straight) or not, and by the general movement path (Table 3.3; behaviors are defined in Section 2.4.2). Schooling behavior was more prevalent during day than night at both study sites (Figure 3.4). At The Dalles Dam during daytime, over 70% of the yearling salmonid events (spring migrants) were schools of three or more fish. Directed movement was

generally more common (> 60%) than non-directed movement during both day and night (Figure 3.5). The lowest percentage of directed movement (46%) was for position 4 near the sluiceway during spring at The Dalles Dam. Movement paths were generally toward the surface flow outlet in all cases except at The Dalles Dam Pos. 4, where paths were mostly right to left (east to west) (Figure 3.6).

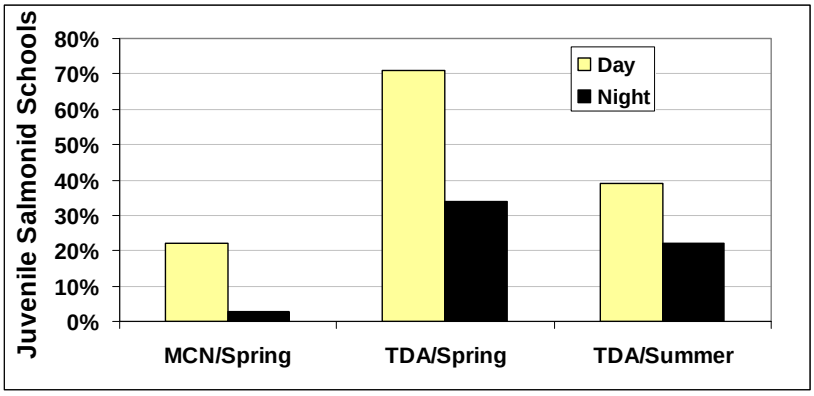

Figure 3.4. Schooling Behavior. Expressed as a percentage of total schools and individuals observed with the DIDSON and calculated separately for day and night during spring and summer at McNary (MCN) and The Dalles (TDA) dams.

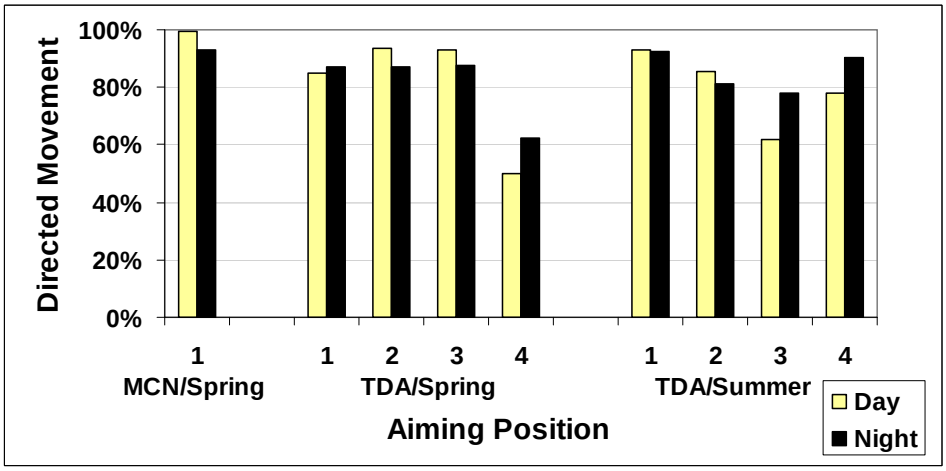

Figure 3.5. Directed Movement Behavior. Expressed as a percentage of total directed and non-directed movement observed with the DIDSON and calculated separately for day and night for each aiming position during spring and summer at McNary (MCN) and The Dalles (TDA) dams. Aiming positions are defined in Figures 2.5 and 2.7.

Table 3.3. Fish Movement Tally Data. Movement variables are defined in Section 2.4.2. The path categories are from the dam looking into the forebay. Aiming positions are in Figures 2.5 and 2.7. Missing periods zero observations.

					Schooling		Directed Movement			Path				
Dam	Season	Period	Aiming Position	n	No School	School	Not Directed	Directed	Milling	Right to Left	Left to Right	Toward SFO	Toward Forebay	Multiple
McNary	Spring	Dawn	1	25	21	4	0	25	0	2	0	23	0	0
		Day	1	529	413	116	2	527	0	92	2	424	5	6
		Dusk	1	97	88	9	1	96	0	15	0	81	1	0
		Night	1	372	362	10	26	346	4	45	2	300	2	19
The Dalles	Spring	Dawn	1	10	7	3	4	6	1	3	1	3	0	2
			2	51	37	14	13	38	1	15	5	19	0	11
			3	75	44	31	18	57	1	2	3	50	3	16
			4	1	0	1	1	0	0	0	0	0	0	1
		Day	1	191	61	130	29	162	6	145	6	14	1	19
			2	400	96	304	25	375	6	103	44	206	0	41
			3	83	37	46	6	77	2	10	22	43	0	6
			4	52	16	36	26	26	0	2	9	17	1	23
		Dusk	2	3	2	1	0	3	0	1	1	1	0	0
		Night	1	62	33	29	8	54	7	45	3	5	0	2
			2	165	92	73	21	144	3	34	9	86	5	28
			3	122	101	21	15	107	1	20	1	86	0	14
			4	16	16	0	6	10	0	0	2	8	0	6
The Dalles	Summer	Dawn	2	2	1	1	0	2	0	0	1	1	0	0
			3	2	2	0	1	1	0	0	0	1	0	1
		Day	1	264	156	108	18	246	9	158	13	66	5	13
			2	199	103	96	29	170	16	80	1	81	6	15
			3	282	166	116	108	174	45	30	3	126	10	68
			4	212	158	54	47	165	11	1	1	167	2	30
		Dusk	1	35	27	8	1	34	1	6	17	7	0	4
			2	4	3	1	0	4	0	0	0	4	0	0
			3	24	20	4	3	21	0	0	0	21	0	3
			4	67	50	17	16	51	2	3	0	42	0	20
		Night	1	66	58	8	5	61	3	24	9	26	0	4
			2	63	57	6	12	51	1	14	3	33	2	10
			3	135	80	55	30	105	5	8	0	96	1	25
			4	82	74	8	8	74	2	1	0	73	0	6
Total				3691	2381	1310	479	3212	127	859	158	2110	44	393

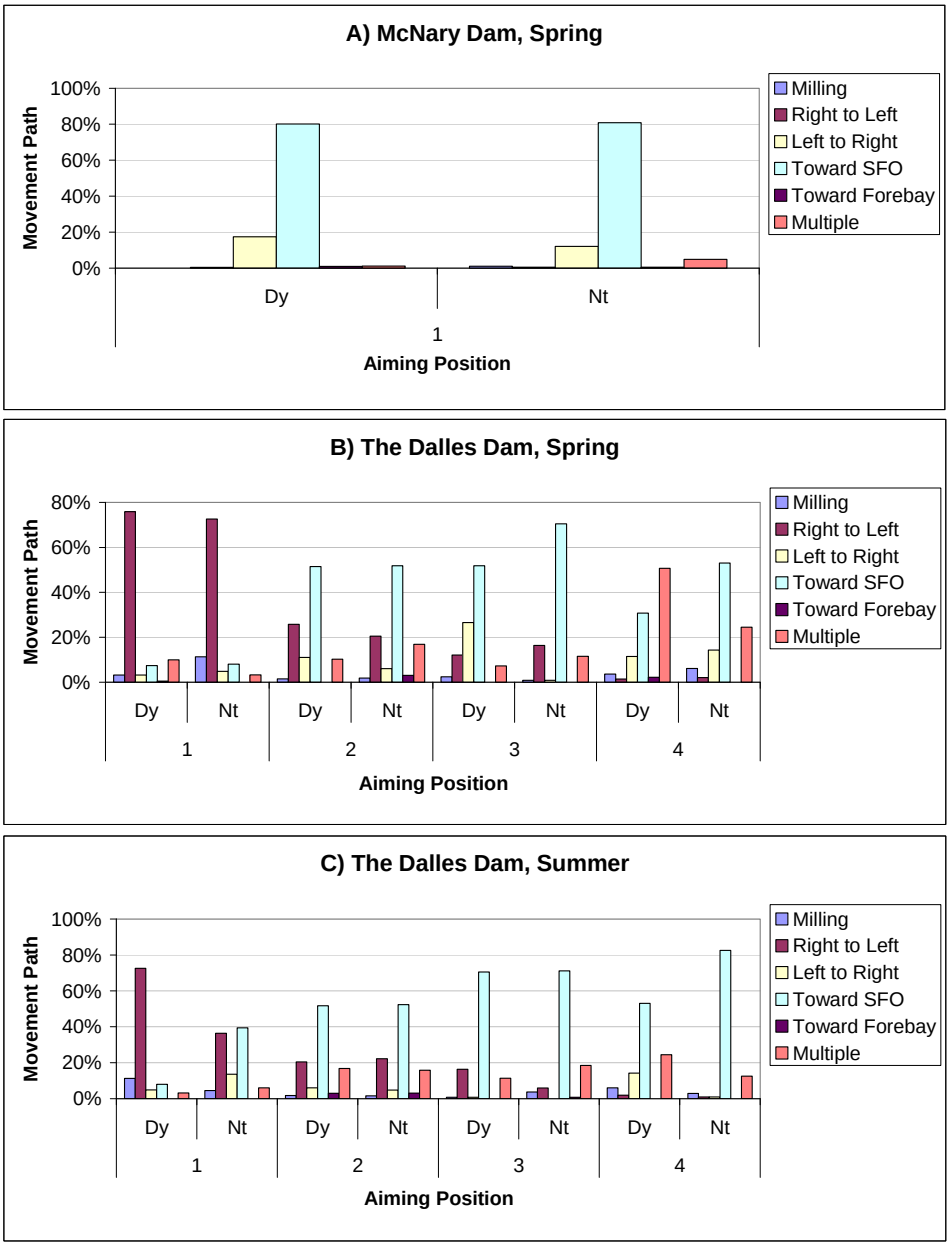

Figure 3.6. Movement Paths. Expressed as a percentage of total movement paths observed with the DIDSON and calculated separately for day and night for each aiming position during spring at McNary Dam (A) and spring (B) and summer (C) at The Dalles Dam. The path categories "Left to Right" and "Right to Left" are from the dam looking perpendicular into the forebay. Aiming positions are defined in Figures 2.6 and 2.8.

3.2.3 Fish Speeds

Using the spring day period as an example, fish speed was highest (> 1.5 m/s) within 5 m of TSW2 during our six-day April sampling period at McNary Dam (Figure 3.7). Fish were generally observed moving at an oblique angle toward the TSW. Observed fish speeds near the Sluice 1-1 and 1-2 entrances were slow, but the direction of movement was usually toward the entrances (Figure 3.7).

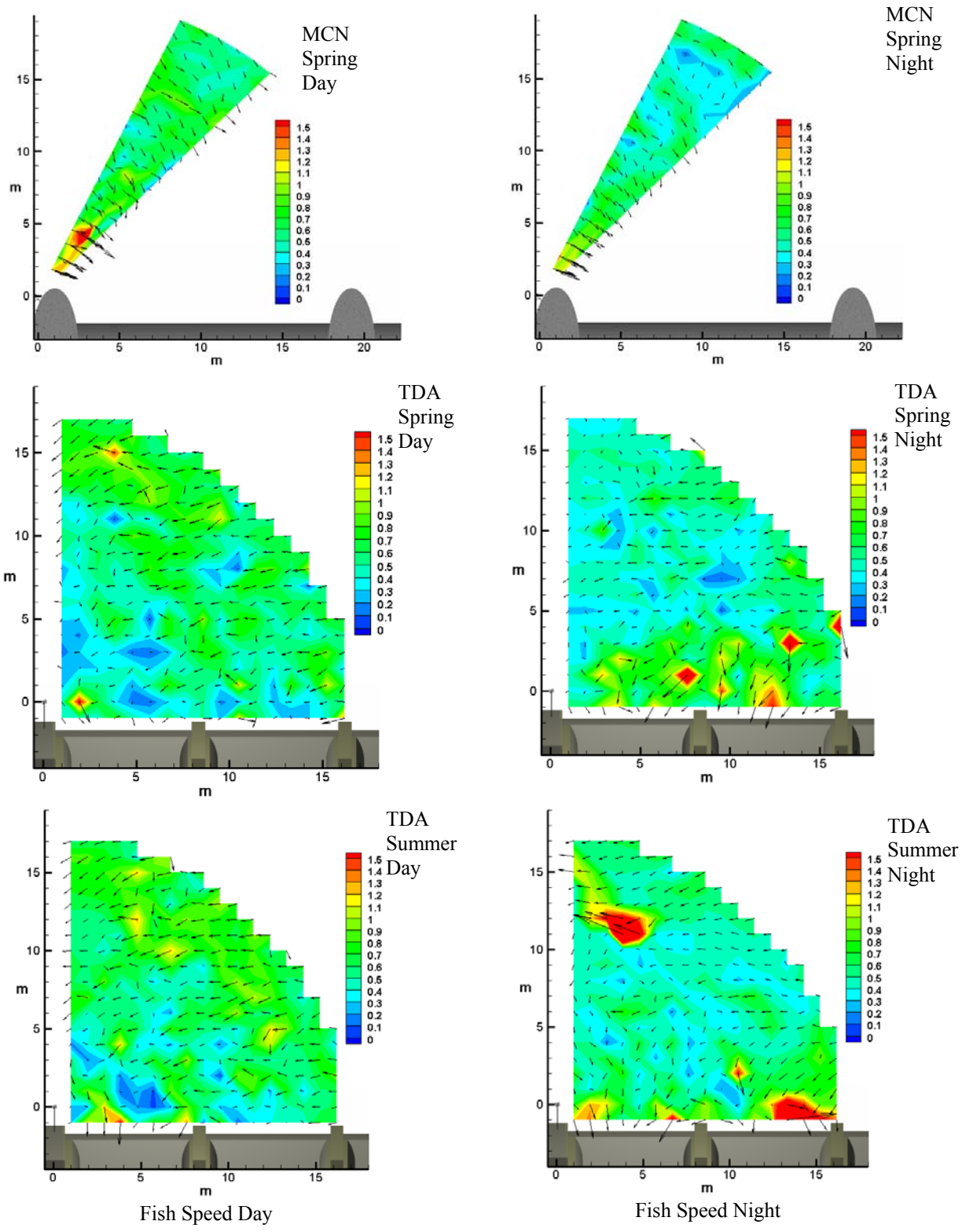

Figure 3.7. Contour and Vector Plots of Observed Fish Speed (m/s).

3.3 Fish Behavior Relative to Hydrodynamics

Observed fish movement is the result of the interaction between the flow field and fish swimming behavior. That is, the observed fish velocity vector is the sum of the water velocity and the fish swimming effort vectors, where theta (θ) is the angle between these two vectors (Figure 3.8). Thus, fish behavior can be characterized by four response variables (see Section 2.4.2 for mathematical definitions):

1. Fish speed (m/s) is the magnitude of the fish velocity vector expressed as displacement per unit time over ground.
2. Fish-swim-effort (m/s) is the magnitude of the fish effort vector.
3. Swim angle (deg) is the angle between the water velocity and fish effort vectors.
4. Effort-cosine-theta (m/s) is the magnitude of the projection of the fish effort vector onto the water velocity vector.

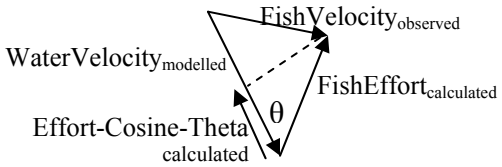

Figure 3.8. Observed Fish and Water Velocity Vectors and the Calculated Fish Swimming Effort Vector along with Swimming Angle (θ) and Effort-Cosine-Theta.

3.3.1 Fish Swimming Behavior Relative to Flow

We used CFD water velocity data and observed fish velocity data from the DIDSON to calculate fish-swimming-effort and effort-cosine-theta to quantify fish behavioral responses relative to the SFO flow nets at The Dalles Dam. Fish-swimming-effort (m/s) is the magnitude of the vector for fish-swimming-effort. Positive values of effort-cosine-theta indicate fish swimming with the flow; negative effort-cosine-theta values indicate fish swimming against the flow.

During our sampling periods, effort-cosine-theta was, on average, negative at The Dalles Dam. Schools had higher effort-cosine-theta values than individuals (Figure 3.9). At The Dalles Dam, the data suggested that schools were swimming into the flow more so than individuals. Differences between day and night for effort-cosine-theta were not evident (Figure 3.9).

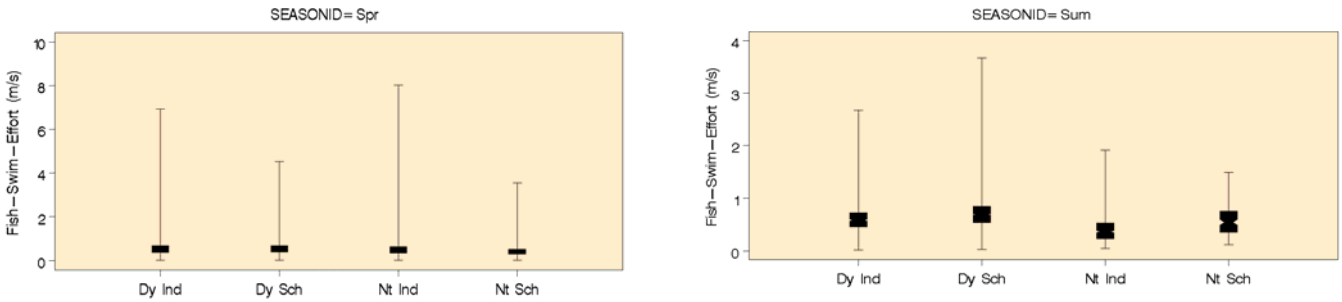

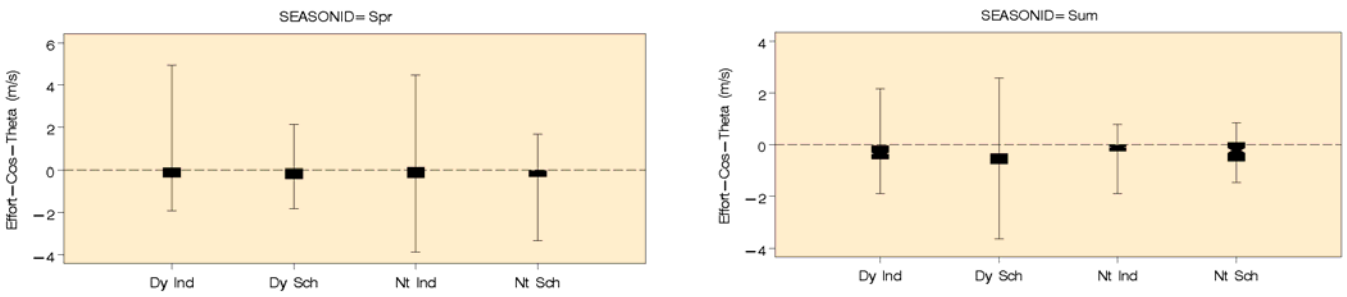

Figure 3.9. Box-Whisker Plots of Fish-Swimming-Effort (m/s) and Effort-Cosine-Theta (m/s) for Individual Fish and Schools by Day/Night. Effort cosine theta values above the reference line (> 0 m/s) indicate fish swimming with the flow and vice versa for swimming against the flow.

Further analysis of fish swimming behavior relative to flow involved using effort-cosine-theta to categorize fish behaviors as: a) passive, b) active swimming against the flow (positive rheotaxis), and c) active swimming with the flow (negative rheotaxis). Passive behavior was defined as being within 0.03 m/s of zero, i.e., about one-fifth of a body length per second. Active behaviors were more prevalent than passive (Figure 3.10). The majority behavior was active swimming *against* the flow (60 to 90%). Conversely, approximately 20-30% of the behavior at The Dalles Dam was active movement *with* the flow. A small fraction of swimming behavior was passive (~5%). Swimming against the flow, or positive rheotaxis, was more common in summer than spring at The Dalles Dam. Generally, individual fish were less likely to swim against the flow than schools of fish. The most dominant fish behavior at The Dalles Dam was active swimming against the flow (Figure 3.10).

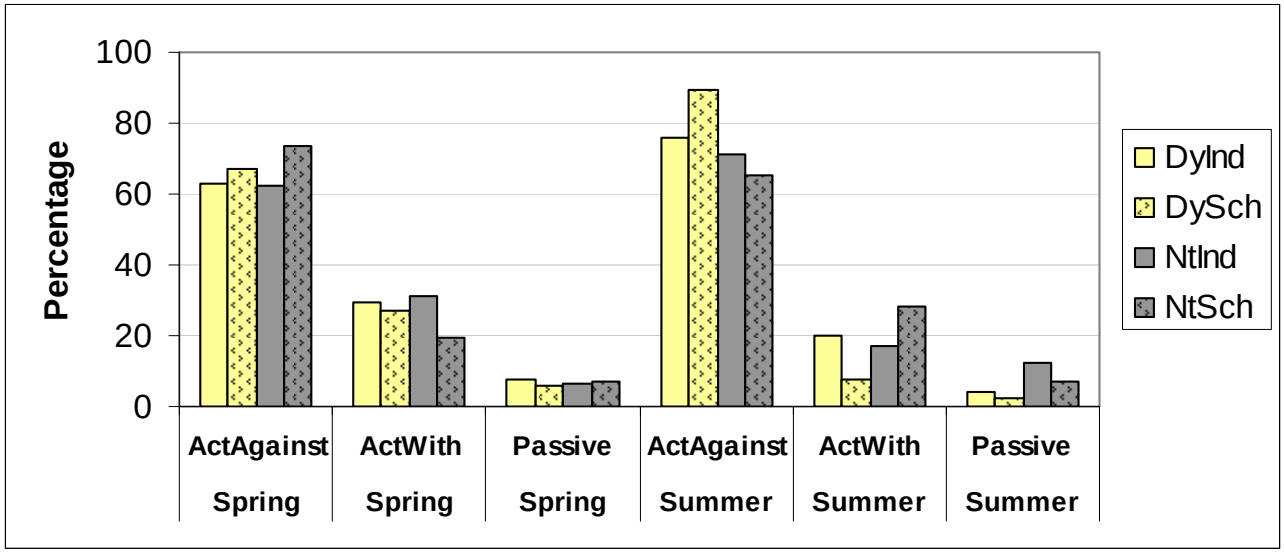

Figure 3.10. Fish Behavior Percentages. Behavior categories are passive, active swimming against the flow, and active swimming with the flow. See text for definitions. Percentages were calculated seasonally for separately for individual fish and schools during day and night, e.g., for spring/day/individuals, the sum of percentages for active against, active with, and passive equals 100.

Fish effort superimposed on flow conditions shows relatively high fish-swim-effort values and negative effort-cos-theta just upstream of the sluice entrances (Figure 3.11). Water velocity increases in this region, as does acceleration and strain. The patterns for fish effort and the hydraulic variable are similar between SL 1-1 and 1-2. Water and fish features are less dynamic at 5 to 20 m away ferom the entrance than they are with 5 m of them.

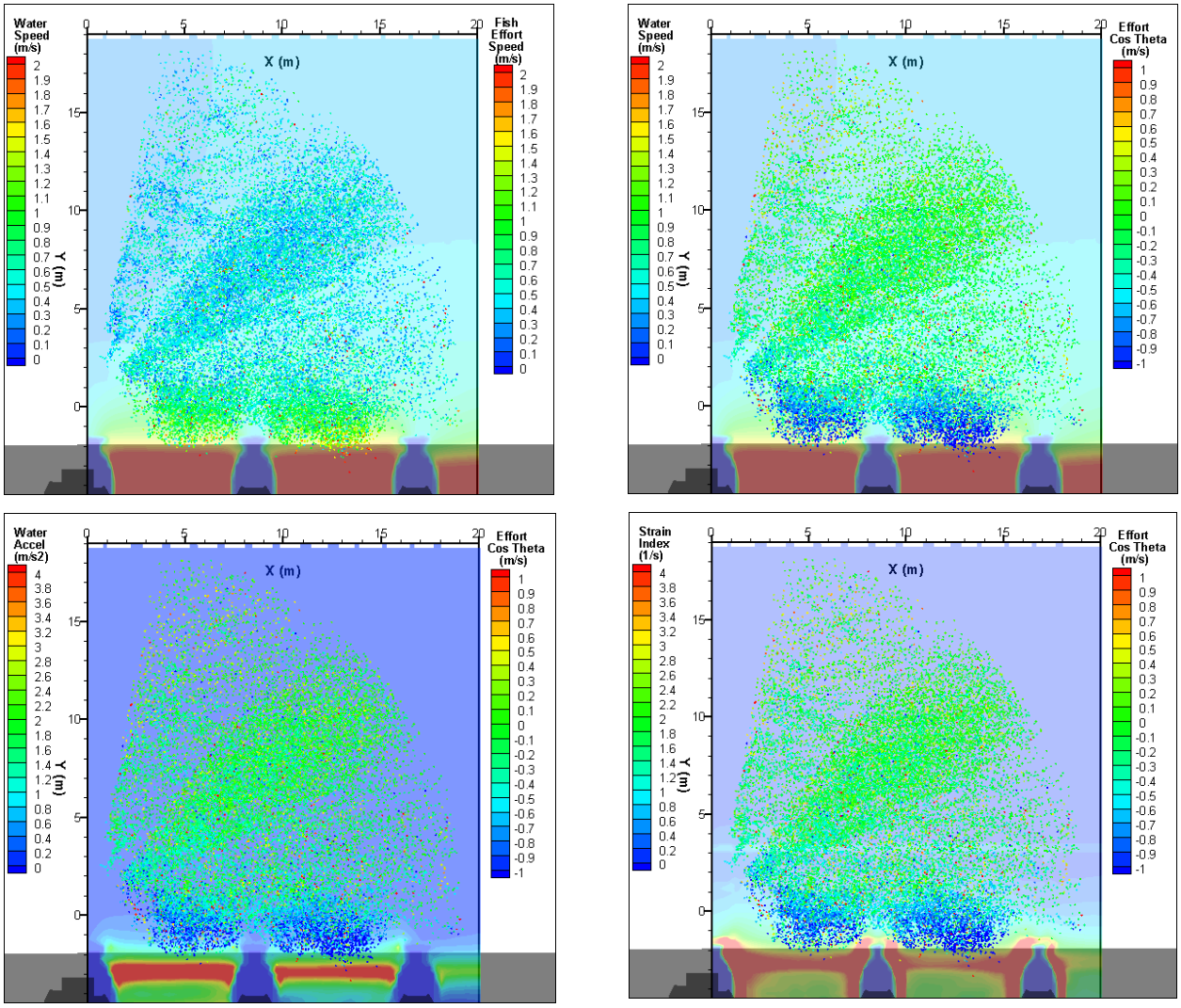

Figure 3.11. Fish-swim-effort and effort-cos-theta are associated with water velocity fields (top row), acceleration field (bottom left), and strain field (bottom right). Hydraulic data are from the CFD simulation. The fish data points are ping-to-ping observations processed from DIDSON output.

3.3.2 Correlation Analysis

The preceding analysis of fish swimming behavior relative to flow was possible because we merged water velocity and fish movement data allowing calculation of fish-swimming-effort and effort-cosine theta. For this same reason, we can perform a correlation analysis of hydraulic variables derived from the water velocity data to elucidate which of these variables contribute most to explaining variation in fish

swimming behavior. Separate correlation analyses were performed for spring and summer to focus on yearling and subyearling migrants, respectively. We also distinguished between individual fish and schools in the analysis.

The correlation matrices for effort-cos-theta had higher correlations with hydraulic variables than did fish-swim-effort (Table 3.4). The highest correlations (0.46-0.47) were between effort-cos-theta and water velocity magnitude, V (water velocity y-component, perpendicular to the dam), W (water velocity vertical-component), total acceleration, and strain. Most of spatial derivatives of velocity were not strongly correlated with the fish behavior variables.

During both spring and summer, the strongest correlations (generally > 0.50) between the fish behavior variables and the hydraulic variables were for fish schools during day (Table 3.5). Individual fish at night during summer had strong correlation coefficients, but the sample size was only 11. Fish-swim-effort and effort-cos-theta for fish schools during day were most strongly associated with velocity magnitude and strain.

Table 3.4. Correlation Matrices between Fish Behavior and CFD Hydraulic Variables for All Data Combined for The Dalles Dam See Section 2.3.2 for variable definitions. Cells with correlation coefficients greater than 0.4 are shaded to ease examination of the table. There were 22,878 data points for each Pearson correlation.

	U	V	W	VelocityMag.	dUdX	dVdX	dWdX	dUdY	dVdY	dWdY
Xeffort	0.04	-0.17	0.16	0.17	-0.13	0.08	-0.06	0.08	0.15	-0.14
Yeffort	0.06	-0.41	0.41	0.41	-0.29	0.07	-0.16	0.12	0.36	-0.37
Fish-Swim-Effort	0.03	-0.36	0.36	0.36	-0.26	0.09	-0.16	0.12	0.33	-0.32
Effort-Cos-Theta	-0.19	0.47	-0.47	-0.46	0.36	-0.04	0.13	-0.10	-0.42	0.42

	dUdZ	dVdZ	dWdZ	AU	AV	AZ	Total Accel.	Strain
Xeffort	0.05	-0.15	-0.16	-0.05	-0.14	0.12	0.15	0.17
Yeffort	0.17	-0.38	-0.39	-0.02	-0.34	0.32	0.34	0.39
Fish-Swim-Effort	0.13	-0.35	-0.35	-0.03	-0.32	0.28	0.32	0.35
Effort-Cos-Theta	-0.26	0.43	0.44	0.00	0.37	-0.37	-0.38	-0.46

Table 3.5. Correlation Matrices between Fish Behavior and CFD Hydraulic Variables Separately for Combinations of Spring and Summer, Day and Night, and Individuals and Schools. See Section 2.3.2 for variable definitions. Cells with correlation coefficients greater than 0.4 are shaded to ease examination of the table. There were 22,878 data points for each Pearson correlation.

	Fish-Swim-Effort				Effort-Cos-Theta			
Spring	DyInd	DySch	NtInd	NtSch	DyInd	DySch	NtInd	NtSch
n	528	1037	285	23	528	1037	285	23
Velocity Mag.	0.38	0.61	0.23	0.18	-0.32	-0.55	-0.32	-0.10
Total Acceleration	0.35	0.56	0.17	-0.11	-0.29	-0.50	-0.25	0.35
Strain	0.39	0.59	0.21	-0.14	-0.29	-0.54	-0.31	0.42
Summer								
n	260	610	11	86	260	610	11	86
Velocity Mag.	0.25	0.50	0.74	0.27	-0.17	-0.54	-0.85	-0.27
Total Acceleration	0.21	0.49	0.71	0.28	-0.17	-0.52	-0.83	-0.26
Strain	0.28	0.49	0.66	0.26	-0.21	-0.53	-0.78	-0.24

3.3.3 Non-Linear Regression Analysis

The purpose of the non-linear regression analysis was to examine quantitative relationships between the fish behavior variables and hydraulic variables to support development of SFO design guidelines. Based on the fish observations (Section 3.2), fish swimming behavior relative to flow (Section 3.3.1), and the correlation analysis (Section 3.3.2), we performed non-linear regression analysis on the high resolution ping to ping data set for The Dalles Dam, separately for individual fish and schools of fish and for spring and summer. We used fish-swim-effort and effort-cos-theta as the response variables because in our view they best reflected fish behavior out of all the fish movement variables. We analyzed separate relationships between the two fish variables and the following hydraulic variables obtained from CFD model results: water velocity magnitude, total acceleration, and strain. Data for individual and schools of fish were combined in this analysis. Log-transforming the independent variables did not make an apparent difference in the shape or pattern in the splines. The findings that follow reflect only the range of conditions during our sampling periods.

For fish-swim-effort as the dependent variable (Figure 3.12), the scatter cloud of data points was oriented in an upward direction as the independent variables increased from their low values during both spring and summer. The corresponding splines reflected this as fish-swim-effort trended upward as velocity, acceleration, or strain increased. For acceleration and strain, the regression curve started to level off at about 0.35 m/s^2 and 1.0 s^{-1}, respectively. For a given independent variable, the spline for spring was generally higher than the corresponding spline for summer, i.e., fish-swim-effort during spring was stronger than that in summer (see Figure 3.12). The data were sparse at larger values of the independent variables.

For effort-cos-theta as the dependent variable (Figure 3.13), the scatter cloud of data points was oriented in a downward direction as the independent variables increased from their low values during

both spring and summer. That is, as velocity, acceleration, or strain increased, fish swimming actively against the flow increased. During sring, effort-cos-theta peaked at approximate velocity 0.9 m/s, acceleration 0.3 m/s^2, and strain 0.95 s^{-1}. During summer, peaks were not observed. Again, the data were sparse at high end for the independent variables.

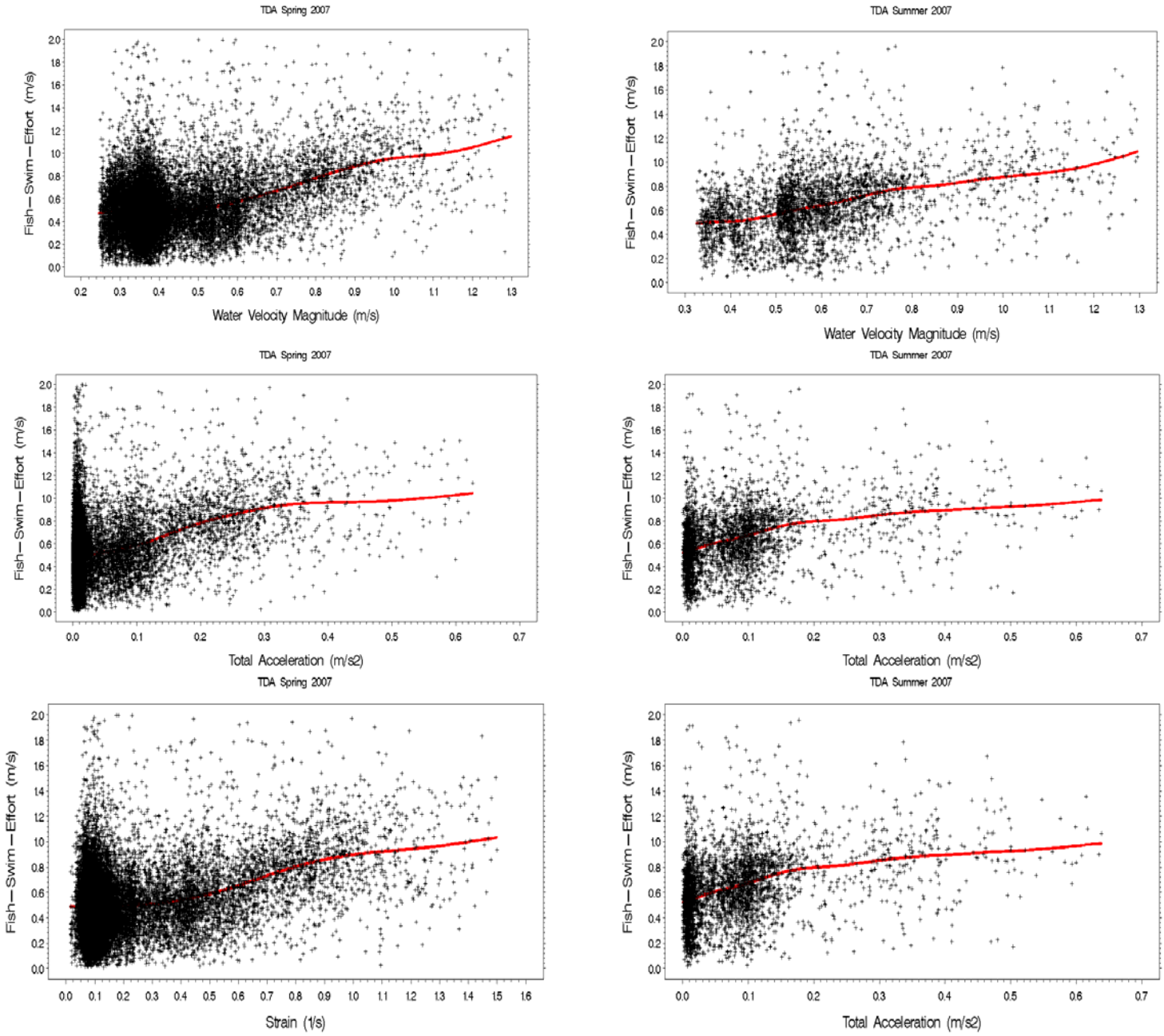

Figure 3.12. Scatterplots with Non-Linear Regression Splines for Fish-Swim-Effort versus Water Velocity Magnitude, Total Acceleration, and Strain at The Dalles Dam during Spring and Summer 2007.

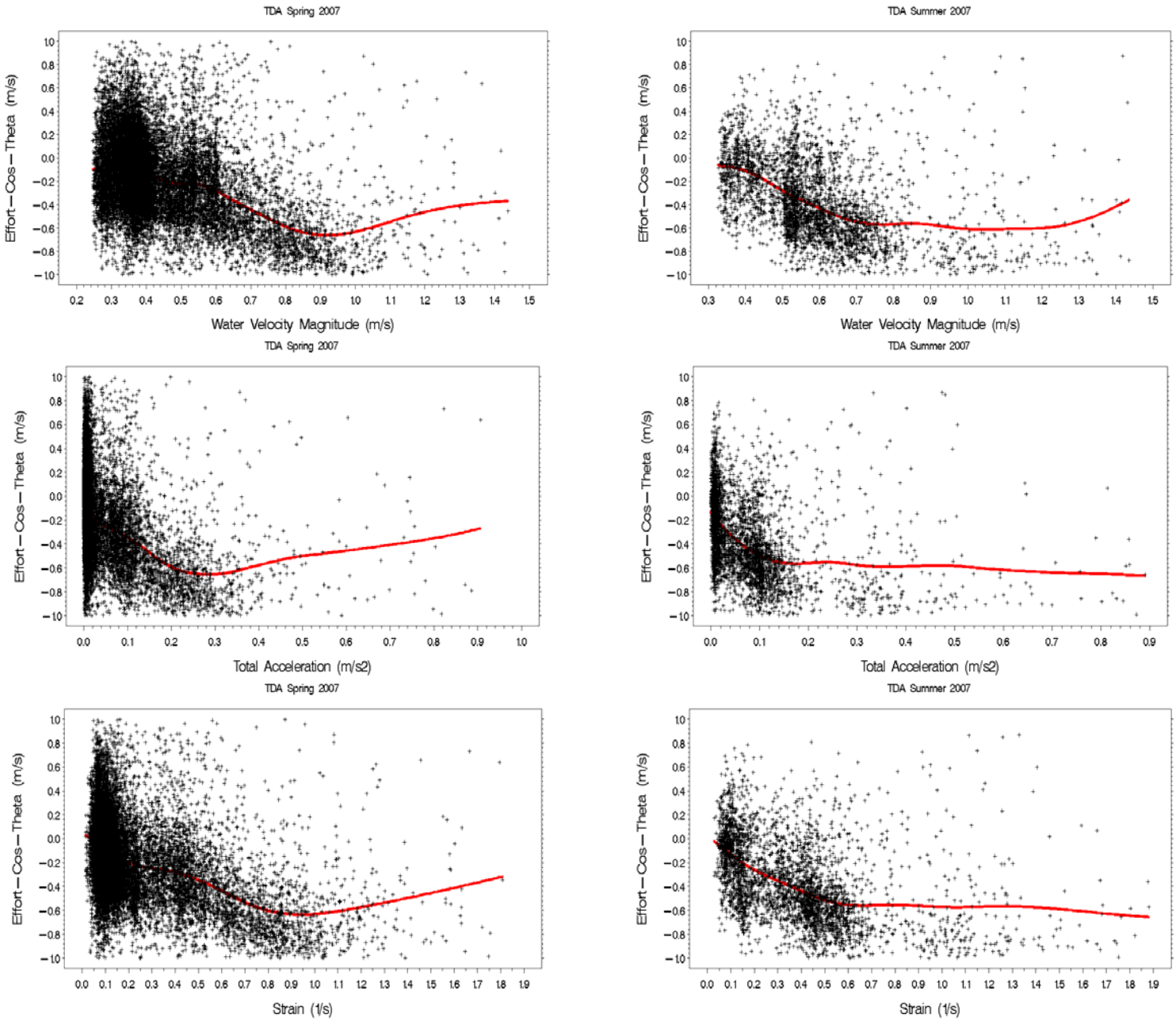

Figure 3.13. Scatterplots with Non-Linear Regression Splines for Effort-Cos-Theta versus Water Velocity Magnitude, Total Acceleration, and Strain at The Dalles Dam during Spring and Summer 2007.

4.0 Discussion

We studied smolt movements and hydrodynamic conditions at surface flow outlets at McNary and The Dalles dams on the Columbia River during spring and summer 2007. Simultaneous ADCP and DIDSON data were collected *in situ* and CFD simulations were performed after the field season. At McNary Dam, a six-day pilot study (April 21-26, 2007) in the nearfield (< 20 m) of a prototype SFO called the Temporary Spillway Weir (TSW2 at Bay 19) was conducted. We established a deployment procedure for the McNary spillway that minimized impact to project activities, collected and analyzed data for 8,574 ping to ping observations on 1,023 fish events. During May 1 to July 12, 2007 at The Dalles Dam, we collected data in the nearfield of the sluiceway SFO to characterize fish behavior and water velocity patterns. From 37,737 ping to ping observations for 2,669 fish events and associated hydraulic conditions at The Dalles Dam.

The comparison of the ADCP and CFD results revealed an apparent problem with our application of the ADCP. The instrument was functioning properly, but the assumption that water currents were sufficiently homogenous for a given range in the ADCP beams may not have been met, producing anomalous water velocity vectors. Therefore, all water-related and fish effort variables were calculated using CFD data.

Comparison with Previous Studies

Johnson et al. (2007) summarized the biological and hydraulic studies at The Dalles Dam sluiceway. The fish behavior results are consistent with previous examinations of fine scale (<1 m) fish movements in the sluiceway flow net using the sonar tracker (Hedgepeth et al. 2002; Johnson et al. 2001) and DIDSON (Johnson et al. 2005b, 2006). Similar water velocity patterns were evident in hydraulic data summarized by Johnson et al. (2007). Other hydraulic variables, such as acceleration and strain, have not typically been calculated or reported.

Previous studies have shown that smolt behavior at The Dalles Dam is directly related to performance of the sluiceway SFO. Smolts congregate at the west end of the dam where open sluice gates are located. In fact, fish concentrations we observed during 2007 were so high that we sub-sampled the data without losing resolution in the behavior patterns. Sluiceway passage efficiencies (relative to the powerhouse) range from 10% to 50% depending on year and season (Johnson et al. 2007). Fish have been observed rejecting the sluiceway entrance (Ploskey et al. 2001); this behavior was noticeable, not simply a rare occurrence. Because some fish approached then swam away from the entrance only to move back down or over to an adjacent portal and pass downstream, the acclimatization concept (Goodwin et al. 2006) appears to apply to passage at The Dalles Dam sluiceway. This would explain the relatively high passage efficiencies despite rejection. An issue, however, is residence time in the forebay. While short relative to other mainstem dams, rejection, milling, or holding behaviors prolong residence time thereby increasing vulnerability to predation. We observed predators at the sluiceway entrance in this study, as we have previously (Johnson et al. 2003). The DIDSON/ADCP approach could be used to study predation at SFO entrances and other structures at mainstem dams. For smolts, the entrainment zone, defined as the area where the probability of passing into a sluiceway entrance is greater than 90%, extends about 6-8 m from the Sluice 1-1 (Johnson et al. 2001, 2004). Observed fish movements within 6 m of the dam from the

study herein were generally toward the sluiceway and are consistent with the entrainment zone determined previously. Studies in 1999 to 2003 and 2004 at the sluiceway used up-looking split-beam transducers to sample fish immediately upstream of the sluiceway sill (Y = 0 to 3 m in our coordinate system) and estimate passage rates into the sluiceway (e.g., Ploskey et al. 2001). Invariably, acoustic detections of fish tracks had to be filtered based on direction of movement. Our results generally corroborate this and other findings from previous studies.

New Information and Management Implications

The new information the 2007 results provide has management implications:

- Schooling behavior was dynamic and prevalent. The implication is that SFO entrance area must be large enough to accommodate fish schools.
- Fish behavior was dependent on distance from the SFO entrance. This supports the notion that SFO flow nets need to be expansive enough spatially to attract smolts despite competing flow fields.
- Passive fish behavior was observed less than 5% of the time in the SFO flow nets we studied, implying that SFO designs cannot rely only on fish following bulk flow.
- Active swimming against the flow was the most common behavioral response. SFO performance evaluations should include a metric for fish swimming effort in SFO flow fields.
- Fish effort variables were correlated with water velocity, acceleration, and strain. The non-linear regressions indicate potential for this approach of merging fish/flow data to lead to SFO design guidelines in the future as the fish/flow dataset is further populated.

These results are limited to the conditions at the study sites during 2007. Additional data from a diversity of sites in multiple years will help increase the applicability of the data and identify universal trends.

Strengths and Weaknesses of the Technical Approach

The simultaneous ADCP/DIDSON sampling method and statistical analysis has advantages and limitations. The principal advantage of using the ADCP is that measurements can be acquired over an entire water volume of interest without having to physically traverse the instrument, as would be required for point measurement devices such as an ADV (acoustic Doppler velocimeter) or LDV (laser Doppler velocimeter). Profiling capability allows for non-intrusive measurements so that the presence of the instrument does not interfere with the DIDSON measurements or introduce an obstruction to flow that might influence fish behavior and performance of the SFO. Disadvantages of the ADCP are the slow sampling speed (1 Hz) and relatively large sampling volume compared to the size of the fish, although this was less of an issue for fish schools. Another disadvantage when sampling inhomogeneous water velocities is the 12-deg separation between ADCP beams especially at the longer ranges. Finally, a most serious disadvantage for our application was that the assumption of homogeneity apparently was not met; we plan to delve deeper into this issue in consultation with the equipment vendor.

With a single DIDSON, fish movements can be measured in only two dimensions of a three-dimensional environment. Most movement immediately upstream of the sluiceway SFO entrances,

however, is in the horizontal plane (X/Y). For example, Johnson et al. (2001) showed streamtraces of fish tracks were horizontal in the sluiceway nearfield and, furthermore, found average smolt velocity was 0.05 m/s toward the west in the X-dimension, 0.05 m/s toward the sluiceway in the Y-dimension, and 0.01 m/s downward in the Z-dimension. Therefore, the horizontal, two-dimensional nature of our data is generally not a drawback. Future studies with a DIDSON could include rotating the instrument 90 deg to sample a vertical plane. However, fish swimming effort could not be estimated in the vertical plane unless we assume it opposes vertical water velocity to keep the fish at a constant depth. Also, other instruments could be considered, such as the active sonar tracker (Hedgepeth et al. 2002) and the scanning multi-beam, which scans the transmit beam, can provide better vertical resolution than the DIDSON.

The fish movement data on a time-scale of about one measurement per second were collected by manual extraction from image files. This process was time consuming but it produced a high quality data set because the observer could be reasonably sure the images were juvenile salmonids. Automatic tracking software could measure fish positions at a higher rate and probably more accurately than the manual tracker, but we would still need to check each fish track for quality. Nonetheless, an automatic tracker is worth consideration.

Furthermore, it is difficult to discern morphological features that might be used to identify taxa of fish in the DIDSON images. We discriminated between juvenile salmonids and non-salmonids based on size and behavior, e.g., large fish milling and then darting toward a school of smolt were assumed to be predators. Some non-salmonids could have been included in the database, although the impact of this was likely small because we sampled during spring and summer when juvenile salmonids are the dominant fish in terms of numbers in our sample zones. Discerning morphological features is easier at the high DIIDSON frequency than the low frequency.

Comparing the two frequencies (low 1MHz versus high 1.2 MHz) for the DIDSON, the tradeoff is basically between range and resolution. For this research, the increased sample volume because of increased range (20 m versus 10 m) at low frequency offset the increase in resolution at the high frequency. We were able to extract useful data from the low frequency images; however, for the purposes of this study, the ADCP sample volume was too large at ranges greater than 10 m. Future studies of this type should use the DIDSON's high frequency.

Although this study focused on fish movements relative to hydrodynamic conditions, other factors not included in the analysis were undoubtedly also stimulating fish movement. For example, we saw fish move in response to predators. Light, sounds, and structures at the dam could also influence behavior. These factors were a likely source of variability in fish movement data that would not be explained by hydrodynamic variables alone.

The Strain-Velocity-Pressure Hypothesis

Goodwin et al. (2006) suggest that smolts are responding to strain, velocity, and pressure (SVP) in an interrelated, complex manner. They offer the SVP hypothesis to explain and model fish movements in dam forebays. Our results indicate that water velocity is associated with fish swimming behavior. This supports the velocity component of the SVP hypothesis. We examined an index of total strain, using the same algorithm as Goodwin et al. (2006), and found it to be correlated with fish-swimming-effort. Our study did not address pressure because we sampled a two-dimensional horizontal plane.

The NFS model has four behavioral responses (our corresponding terminology is in parentheses): 1) null – follow flow (passive); 2) wall-bounded flow gradient, swim towards the flow vector (active with the flow); 3) free-shear flow gradient, swim against the flow vector (active against the flow), and 4) pressure gradient (not included in our study). These categories are useful to frame behavioral studies of smolt response to hydrodynamic conditions. Fish swimming strongly (to be defined) against the flow could indicate an adverse hydraulic condition. Fish swimming with the flow could indicate favorable conditions, or the fish has simply become negatively rheotactic.

An important element of the SVP hypothesis is acclimatization. Acclimatization is the process of becoming accustomed to new surroundings or circumstances. Our analysis did not and could not account for acclimatization of fish to hydrodynamic conditions. We did, however, observe fish schools initially reject then ultimately pass into the sluiceway. This could be interpreted as acclimatization. Assuming acclimatization is part of the variability in the data, such variability is obvious in scatterplots of fish effort variables in relation to hydraulics.

SFO Reviews

Numerous authors have addressed the issue of establishing hydraulic conditions for the flow nets of SFOs that are conducive to ready passage of downstream migrant juvenile salmonids. The region of interest is called the Decision Zone in the SFO framework proposed by Johnson and Dauble (2006) and modified by Sweeney et al. (2007). A basic premise of the SFO framework is that "SFO entrance conditions…do not consistently and repeatedly elicit an avoidance response before the fish are entrained" (Sweeney et al. 2007). Defining such conditions empirically in hydraulic terms has been a difficult proposition. This is one reason for the modeling approach taken by Goodwin et al. (2006). Authors sometimes use general terms to describe favorable hydraulic conditions. Johnson and Dauble (2006) recommended there not be "localized intense water particle acceleration zones." Johnson et al. (2005) advocated a "gradual increase in water velocity" along the 1 m/s per meter guideline of Haro et al. (1998), one of the few studies to directly address favorable hydraulic conditions, in this case for juvenile Atlantic salmon and shad. Sweeney et al. (2007) suggested that a "reference point" of 1 m/s^2 for acceleration. Reference points were used to identify differences among suites of features among various SFOs; they were not purported to be design criteria. They also recommended smooth acceleration and entrance velocity greater than 2 m/s. The intent of our work ultimately is to define hydraulically conditions for SFO flow nets that are conducive to passage by juvenile salmonids.

SFO Design Guidelines

Statistical associations between juvenile salmonid movements and hydraulic conditions immediately upstream of the sluiceway SFO entrances showed that water speed and acceleration were important variables associated with fish swimming data. We applied a non-linear regression spline technique to extract one-to-one relationships between fish swimming effort and effort-cosine-theta as response variables and water speed, total acceleration, and strain as independent variables. Our premise was that such relationships, however, would be useful to design engineers if the relationships could be properly established and couched. That is, it would be desirable to establish maximum or plateau levels of fish responses. The spline, or estimation of a smooth curve through the data, served as a summary of the scatterplots relating variables. The smoothing splines filtered out local variability allowing a view of the

underlying trend. However, the smoothing spline approach does not describe abrupt or structural relationships (Seber and Wild 1989). Because the level of smoothing was chosen "ad hoc" different smooth curves could have been fit with other choices of smoothing. Therefore, further work is needed to develop this line of analysis although the initial results presented herein are enlightening and indicate the approach is promising.

We presented bi-variate relationships (the non-linear regression splines) to provide insight into fish response to particular hydraulic variables that engineers can use for guidance during SFO design. Smolts, however, are not responding in a one-to-one manner to their hydraulic environment. They are reacting to multiple stimuli in a complex hydrodynamic environment like the nearfield of an SFO. Real-world relationships between smolt responses and hydrodynamic conditions, therefore, are not mutually exclusive, one-to-one associations. The splines, at this time, are not meant to be design *criteria* because it is clear they are increasing at the upper range of our data and did not reveal a distinct plateaus indicative of thresholds. However, the data indicate the potential for this analytical approach to lead to SFO design guidelines in the future. This approach to SFO design guidelines would be strengthened with more diverse, wider ranging water/fish data from multiple SFOs. The comparison of results from the McNary TSW and The Dalles sluiceway serves as an example of different hydraulic conditions and fish behaviors at different sites. We are optimistic that an expanded data set could lead to SFO design guidelines.

Conclusion

Analyzing merged fish/flow data from a diversity of sites in multiple years will strengthen the relationships between smolt responses and hydrodynamic conditions such that universal trends may emerge to support bioengineering efforts aimed at protecting juvenile salmonids.

5.0 Literature Cited

Adams, N. S., D. W. Rondorf, and M. A. Tuell. 1998. Migrational characteristics of juvenile spring chinook salmon and steelhead in the forebay of Lower Granite Dam relative to the 1997 surface bypass collector tests. Final report for 1997 submitted to U.S. Army Corps of Engineers, Walla Walla District. Project No. E 86930151.

Belcher, E. O., H. Q. Dinh, D. C. Lynn, T. J. Laughlin. 1999. Beamforming and imaging with acoustic lenses in small, high-frequency sonars. Proceeding of Oceans '99 Conference, 13-16 September.

CD-Adapco. 2007. User Guide, STAR-CD Version 4. CD Adapco Group, http://www.cd-adapco.com.

Cook C. B., M. C. Richmond, and J. A. Serkowski. 2007. Observations of Velocity Conditions near a Hydroelectric Turbine Draft Tube Exit using ADCP Measurements. Flow Measurement and Instrumentation 18:148-155.

Dauble, D., S. Anglea, and G. Johnson. 1999. Surface flow bypass development in the Columbia and Snake rivers and implications to Lower Granite Dam. Final report submitted to U.S. Army Corps of Engineers, Walla Walla District. July 21, 1999.

Goodwin, R. A., J. M. Nestler, J. J. Anderson, L. J. Weber, and D. P. Loucks. 2006. Forecasting 3-D fish movement behavior using a Eulerian-Lagrangian agent method (ELAM). Ecological Modeling 192:197-223.

Gordon, R. L. 1989. Acoustic measurement of river discharge. Journal of Hydraulic Engineering-ASCE 115(7):925-936.

Haro, A., M. Odeh, J. Noreika, and T. Castro-Santos. 1998. Effect of water acceleration on downstream migratory behavior and passage of Atlantic salmon smolts and juvenile American shad at surface bypasses. Transactions of the American Fisheries Society 127:118-127.

Hedgepeth, J. B., G. E. Johnson, A. E. Giorgi, and J. R. Skalski. 2002. Sonar tracker evaluation of fish movements relative to J-occlusions at The Dalles Dam in 2001. Final report submitted to U.S. Army Corps of Engineers, Portland District.

Johnson, G. E. 1996. Fisheries research on phenomena in the forebay of Wells Dam in spring 1995 related to the surface flow smolt bypass. Final report submitted to U.S. Army Corps of Engineers, Walla Walla District.

Johnson, G. E. and A. E. Giorgi. 1999. Development of surface flow bypasses at Bonneville dam: a synthesis of data from 1995 to 1998 and a draft M&E plan for 2000. Final report submitted to the U.S. Army Corps of Engineers, Portland District, by BioAnalysts, Inc., Battle Ground, WA.

Johnson, G. E. and T. J. Carlson. 2001. Monitoring and evaluation of the prototype surface collector at Bonneville First Powerhouse in 2000: synthesis of results. Final report submitted to the U.S. Army Corps of Engineers, Portland District, by BioAnalysts, Inc., Battle Ground, WA and pacific Northwest national Laboratory, Richland, WA.

Johnson, G. E. and D. D. Dauble. 2006. Surface flow outlets to protect juvenile salmonids passing through hydropower dams. Reviews in Fisheries Science 14:213-244.

Johnson, G. E., A. E. Giorgi, and M. W. Erho. 1997. Critical assessment of surface flow bypass deve my Corps of Engineers, Walla Walla District. April 30, 1997.

Johnson, G. E., J. B. Hedgepeth, A. E. Giorgi, and J. R. Skalski. 2001. Evaluation of smolt movements using an active fish tracking sonar at the sluiceway surface bypass, The Dalles Dam, 2000. Final report submitted to the U.S. Army Corps of Engineers, Portland District, by BioAnalysts, Inc., Battle Ground, WA.

Johnson, G. E., M. E. Hanks, J. B. Hedgepeth, B. D. McFadden, R. A. Moursund, R. P. Mueller, and J. R. Skalski. 2003. Hydroacoustic evaluation of turbine intake J-occlusions at The Dalles Dam in 2002. Prepared by Battelle Memorial Institute for the U.S. Army Corps of Engineers, Portland District, Portland, Oregon, USA. PNWD-3226.

Johnson, G. E., J. B. Hedgepeth, J. R. Skalski, and A. E. Giorgi. 2004. A Markov chain analysis of fish movement to determine entrainment zones. Fisheries Research 69:349-358.

Johnson, G. E., S. M. Anglea, N. S. Adams, and T. O. Wik. 2005a. Evaluation of the prototype surface flow bypass for juvenile salmon and steelhead at the powerhouse of Lower Granite Dam, Snake River, Washington, 1996-2000. N. Amer. J. Fish. Management 25:138-151.

Johnson G. E, M. E. Hanks, F. Khan, C. B .Cook, J. B. Hedgepeth, R. P. Mueller, C. L. Rakowski, M. C. Richmond, S. L. Sargeant, J. A. Serkowski, and J. R. Skalski. 2005b. Hydroacoustic Evaluation of Juvenile Salmonid Passage at The Dalles Dam in 2004. PNNL-15180, Pacific Northwest National Laboratory, Richland, WA.

Johnson, G. E., F. Khan, J. B. Hedgepeth, R. P. Mueller, C. L. Rakowski, M. C. Richmond, S. L. Sargeant, J. A. Serkowski, and J. R. Skalski. 2006. Hydroacoustic Evaluation of Juvenile Salmonid Passage at The Dalles Dam Sluiceway, 2005. Final report submitted to the Corps of Engineers, Portland District by Pacific Northwest National Laboratory, Richland, Washington. PNNL-15540.

Johnson, G., J. Beeman, I. Duran, and A. Puls. 2007. Synthesis of juvenile salmonid passage studies at The Dalles Dam, Volume II: 2001-2005. Final report submitted to the U.S. Army Corps of Engineers Portland District by the Pacific Northwest National Laboratory and the U.S. Geological Survey. PNNL-16443.

Johnson, L., C. Noyes, and G. E. Johnson. 1982. Hydroacoustic evaluation of the efficiency of the Ice Harbor Dam ice and trash sluiceway for passing downstream migrating juvenile salmon and steelhead, 1982. Volume I. Final report submitted to U.S. Army Corps of Engineers, Walla Walla District.

Johnson, R. L. and six co-authors. 2001. Hydroacoustic evaluation of fish behavior at Bonneville Dam First Powerhouse: 2000 prototype surface flow bypass. Final report Final report submitted to the Corps of Engineers, Portland District by Pacific Northwest National Laboratory, Richland, Washington.

Johnson, R. L.; Daly, D. S.; Redgate, T.; Hoffman, A., and Carlson, T. J. 1995. A model to describe smolt behavior during approach to surface collector prototypes, The Dalles Dam, spring 1995. Draft report submitted to the Corps of Engineers, Portland District by Pacific Northwest National Laboratory, Richland, Washington.

Johnson, R., D. Daly, and G. Johnson. 1998. Combining hydroacoustics, flow models to study fish behavior. Hydro Review 18:42-56.

National Oceanic and Atmospheric Administration (NOAA). 2008. Biological Opinion – Consultation on Remand for Operation of the Federal Columbia River Power System, 11 Bureau of Reclamation Projects in the Columbia Basin and ESA Section 10(a)(1)(A) Permit for Juvenile Fish Transportation Program. National Marine Fisheries Service (NOAA Fisheries) - Northwest Region, Seattle, Washington (May 5, 2008).

Nichols, D. W. and B. H. Ransom. 1981. Development of The Dalles Dam trash sluiceway as a downstream migrant bypass system, 1980. Oregon Department of Fish and Wildlife. Portland, Oregon.

Ploskey G., T. Poe, A. Giorgi, and G. Johnson. 2001. Synthesis of Radio Telemetry, Hydroacoustic, and Survival Studies of Juvenile Salmon at The Dalles Dam (1982-2000). PNWD-3131, Battelle Pacific Northwest Division, Richland, Washington.

Ploskey, G. R., M. A. Weiland, C. R. Schilt, J. Kim, P. N. Johnson, M. E. Hanks, D. S. Patterson, J. R. Skalski, and J. Hedgepeth. 2005. Hydroacoustic evaluation of fish passage through Bonneville Dam in 2004. PNNL-15249, Pacific Northwest National Laboratory, Richland, Washington.

Rakowski, C. L., M. C. Richmond, J. A. Serkowski, and G. E. Johnson. 2006. Forebay Computational Fluid Dynamics Modeling for The Dalles Dam to Support Behavior Guidance System Siting Studies . PNNL-15689, Pacific Northwest National Laboratory, Richland, WA.

RDI. 1996. Acoustic Doppler Current Profiler: Principles of Operation. Teledyne RD Instruments, Inc., San Diego, California.

RDI. 1998a. ADCP Coordinate Transformation: Formulas and Calculations. Teledyne RD Instruments, Inc., San Diego, California.

RDI. 1998b. Workhouse Technical Manual. Teledyne RD Instruments, Inc., San Diego, California.

Scheibe, T. D. and M. C. Richmond. 2002. Fish Individual-based Numerical Simulator (FINS): A particle-based model of juvenile salmonid outmigration and dissolved gas exposure history in the Columbia River Basin. Ecological Modeling, 147(3): 233-252.

Schott F. 1987. Medium-range vertical acoustic Doppler current profiling from submerged buoys. Deep Sea Research Part A - Oceanographic Research 33(10):1279-1292.

Seber and Wild. 1989.

Sokal, R. R. and F. J. Rohlf. 1981. Biometry. W.H. Freeman and Company, San Francisco, CA.

Sweeney, C., R. Hall, A. Giorgi, M. Miller, and G. Johnson. 2007. Surface bypass program comprehensive review report. Final report submitted to the U.S. Army Corps of Engineers. ENSR Document No. 09000-399-0409.

Willis, C. F. and B. L. Uremovich. 1981. Evaluation of the ice and trash sluiceway at Bonneville Dam as a bypass system for juvenile salmonids, 1981. Oregon Dep. Fish. Wildl. Annual progress report prepared for the U.S. Army Engineer District, Portland, Oregon.

Appendix A Data Processing and Analysis Methods

A.1 Data Processing

A.1.1 ADCP

As shown in Figures 2.2, 2.3, and 2.4, each ADCP measurement consists of four one-dimensional (one-dimensional) water velocity profile measurements along the axis of each acoustic beam. Only the small volume of water in the measurement cell (0.25-m in this case) because the acoustic beam emitted by each transducer is intentionally focused and narrow. These one-dimensional beam velocities (Beam 1 through Beam 4 in Figure A.1) form the beam coordinate system and are used to derive a three-dimensional (three-dimensional) velocity vector with components (U,V,W) oriented in an instrument coordinate system (Figure A.1). In addition, the velocities in the instrument coordinate system can be transformed to a dam coordinate system where the x-axis is along dam face, the y-axis is oriented perpendicular into the forebay, and the z-axis is the vertical coordinate (Figure A.1).

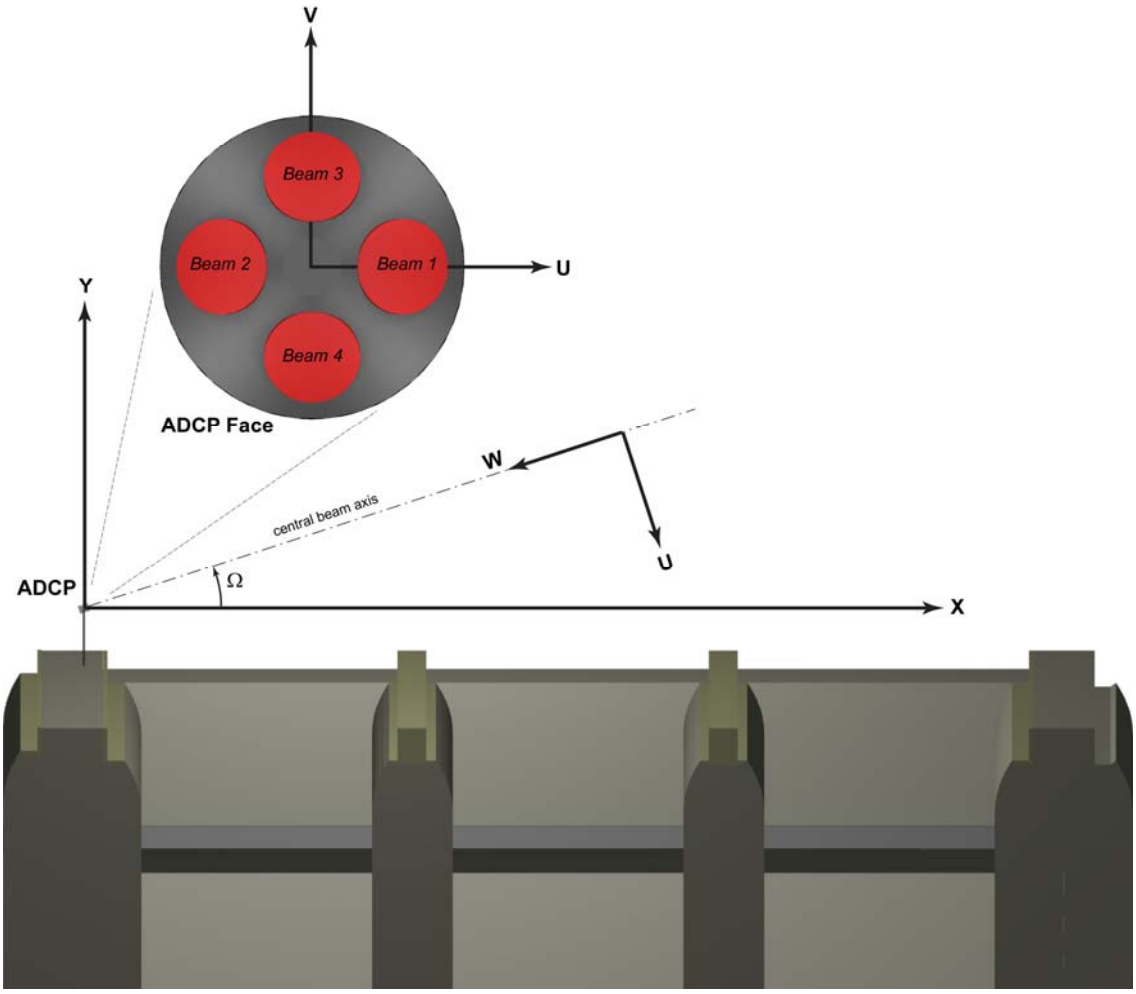

Figure A.1. The ADCP velocity (U, V, W) and the Dam Coordinate Systems. The inset shows the four individual acoustic beams.

Assuming that water currents are homogeneous in the plane perpendicular to the instrument axis, the four one-dimensional beam profile measurements can be combined to compute a profile of three-dimensional water velocities (RDI 1998). The first step is to project the instrument coordinate velocity components (U, V, W) onto the beam coordinates and obtain:

$$\begin{cases} B1 = U\sin\theta + W\cos\theta \\ B2 = -U\sin\theta + W\cos\theta \\ B3 = -V\sin\theta + W\cos\theta \\ B4 = V\sin\theta + W\cos\theta \end{cases} \quad \text{Equation 1}$$

where, θ is the angle between the ADCP beams and the instrument axis. It is equal to 6 degrees for the instrument used in this study. It should be noted that beam coordinates cannot be directly projected into instrument coordinate because beam coordinate system is not orthogonal.

The 4-beam solution for velocity components in instrument coordinates is then

$$\begin{cases} U = \dfrac{1}{2\sin\theta}(B1 - B2) \\ V = \dfrac{1}{2\sin\theta}(B4 - B3) \\ W = \dfrac{1}{4\cos\theta}(B1 + B2 + B3 + B4) \end{cases} \quad \text{Equation 2}$$

Because only three beams are necessary to compute a three-dimensional water velocity with a Janus-configured ADCP, the fourth beam velocity measurement is used for redundancy and to check the reliability of the homogeneity assumption. This error velocity is defined as the difference between the two estimates of W,

$$Er = W_1 - W_2 = \frac{1}{2\cos\theta}(B1 + B2) - \frac{1}{2\cos\theta}(B3 + B4) = \frac{1}{2\cos\theta}(B1 + B2 - B3 - B4) \quad \text{Eq. 3}$$

A set of velocities can also be computed using sets of 3-beams. The 3-beam solutions can be obtained by solving the corresponding beam components in Equation 1. For example, if beams 1-2-3 are used, the solution is

$$\begin{cases} U_{123} = \dfrac{1}{2\sin\theta}(B1 - B2) \\ V_{123} = \dfrac{1}{2\sin\theta}(B1 + B2 - 2B3) \\ W_{123} = \dfrac{1}{2\cos\theta}(B1 + B2) \end{cases} \quad \text{Equation 4}$$

If beams 1-2-4 are used, the solution is

$$\begin{cases} U_{124} = \dfrac{1}{2\sin\theta}(B1 - B2) \\ V_{124} = \dfrac{1}{2\sin\theta}(-B1 - B2 + 2B4) \\ W_{124} = \dfrac{1}{2\cos\theta}(B1 + B2) \end{cases} \qquad \text{Equation 5}$$

The differences of velocity estimates using different 3-beam solution are a function of error velocity. For example, the differences of velocity estimates between 1-2-3 and 1-2-4 are

$$\begin{cases} U_{123} - U_{124} = 0 \\ V_{123} - V_{124} = \dfrac{1}{\sin\theta}(B1 + B2 - B3 - B4) = 2Er\cot\theta \\ W_{123} - W_{124} = 0 \end{cases} \qquad \text{Equation 6}$$

Velocity components in dam coordinates (Velx, Vely, and Velz) are computed by transforming the velocity components in instrument coordinates (Figure A.1). In this study, the ADCP was placed almost horizontally with only a 1.2 degree downward angle into the water, the transformation could be simplified as:

$$\begin{cases} Vel_X = U\sin\Omega - W\cos\Omega \\ Vel_Y = -U\cos\Omega - W\sin\Omega \\ Vel_Z = V \end{cases} \qquad \text{Equation 7}$$

where Ω is angle from the dam face to the ADCP instrument axis (see Figure 2.12).

Because of the very small cell size (0.25-m) and fast sampling frequency (1 Hz) used for data acquisition, different running averaging filters were applied to the ADCP measurements to filter out noise. Figure A.2 shows the effect of using three different time-averaging windows on the root mean square ADCP velocity. A 30-second running-average was selected as a good compromise between reducing noise in the raw 1-Hz data and excessive by comparing with the root-mean-square velocities obtained by an Acoustic Doppler Velocimeter (ADV) upstream of a Tainter gate at The Dalles Dam Spillway (Mark Weiland, personal communication).

The filtered velocity measurements were then used to derive indices for use in the merged analysis of fish response and hydrodynamics. Hydrodynamic variables included velocity, root-mean-square velocity (turbulence index), time derivative of velocity (acceleration index), and the spatial gradient of velocity (shear index). Spatial and temporal changes (derivatives) were calculated using second-order central difference scheme.

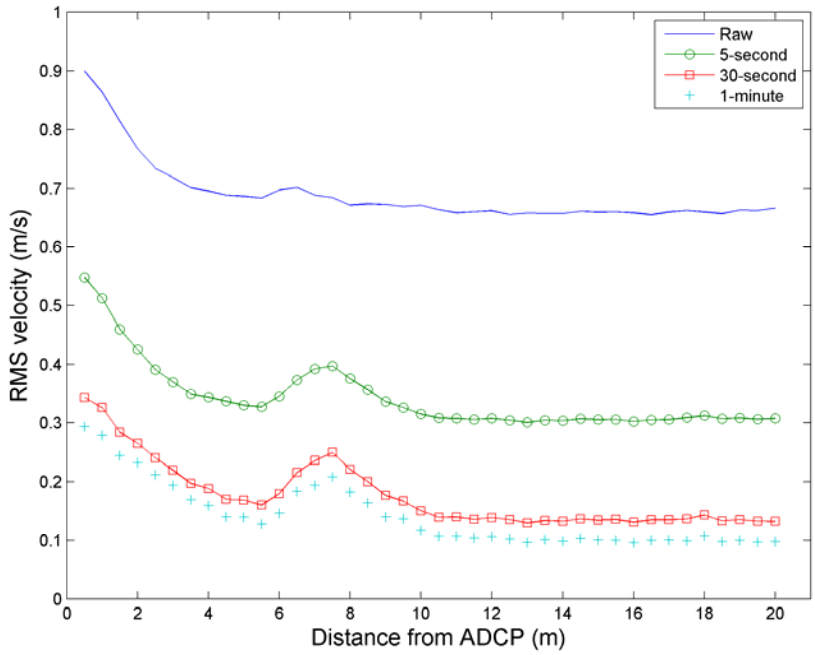

Figure A..2. Filtering the Root-Mean-Square ADCP Velocity Measurements Using Different Running Averaging Filters.

A.1.2 DIDSON

The DIDSON data files collected in the field were processed at PNNL offices in Richland and Sequim, Washington. Processing involved two steps -- behavioral tallying and manual tracking. By definition, an "event" is an observation of behavior through time from the DIDSON acoustic images. An event can be a school of fish or an individual fish.

Behaviors were tallied during playback of the DIDSON files. Researchers watched fish images on the computer screen and systematically noted behaviors for each event on a spreadsheet according to the following categories. Predation and large fish events were noted but not used in the analysis. These data were collected at the fish event level.

- Schooling – no (1 or 2 fish) or yes (> 2 fish)
- Directed Movement – yes (movement straight through the sample volume) or no (meandering movement)
- Path – for The Dalles – direction of movement was milling, east to west, west to east, toward sluice, toward forebay, or multiple; for McNary -- milling, north to south, south to north, toward TSW, toward forebay, or multiple

The events, both individual fish and fish schools, identified during the behavior tally process were manually tracked using custom software developed in our previous DIDSON studies. We used the Visual Basic manual tracker program that was developed and applied in 2004 (Johnson et al. 2005) to extract

spatial information from tracks of individuals and schools of fish recorded in binary files of the DIDSON acoustic camera. The program interactively identified fish tracks by boxing around fish in each frame display using a mouse pointer. We typically manually tracked once every 7 pings of data in an event. The relative coordinates of the box's opposite corners were recorded in ASCII data files with the binary track file name, frame number, date, time, pan angle, number of fish in box and a unique track identification number. From the manual tracking step, the primary data for each event were time and two-dimensional (x,y) position relative to the dam. Positional data, which were transformed in Oregon State Plane North coordinates (NAD 27), are called ping to ping data.

We combined the event-level behavioral tally data and the ping to ping positional data to produce the fish data set. It was merged with the hydraulic data set resulting from processing the ADCP data.

A.1.3 CFD

Using the CFD output, effort, strain index, acceleration magnitude and effort cos theta were all calculated in Tecplot using equations described in Section 2.4.2. Water variables were interpolated from a slice through the volume using Tecplot onto fish positions using inverse distance extrapolation (exponent =3.5, octant, 8 points). This slice was made at 46.67 m (153 ft). Most merging was done in Tecplot. ID, date and time were added in Excel.

A.1.4 Merging

Merging refers to the combining of the ADCP data and fish position data and the calculation of the combination observations of fish effort based on water and fish velocities. The derived ADCP velocity measurements were merged by time with fish positions recorded by the DIDSON using date and time resolved to closest hundredth of a second. During the merger, some of the ADCP hydrodynamic variables that were computed with respect to range were transformed to dam coordinates. DIDSON fish coordinates were also transformed to dam coordinates centered at the DIDSON origin and where the X-axis lies parallel to the dam, the Y-axis is perpendicular away from the dam and the Z-axis points vertically with positive up. Variables that were transformed included fish position, range derivative of root-mean-square velocity (turbulence index), and the spatial gradient of velocity (shear index). Prior to merger, the ADCP positions were recalculated to reflect a coordinate system positioned at the DIDSON origin.

The transformations of range derivatives of root-mean-square velocity ($U'_{rms}, V'_{rms}, W'_{rms}$) were

$$\frac{\partial U'_{rms}}{\partial x} = \frac{\partial U'_{rms}}{\partial r}\frac{dr}{dx} = \frac{\partial U'_{rms}}{\partial r}\frac{1}{\cos\theta}$$

$$\frac{\partial U'_{rms}}{\partial y} = \frac{\partial U'_{rms}}{\partial r}\frac{dr}{dy} = \frac{\partial U'_{rms}}{\partial r}\frac{1}{\sin\theta}$$

where θ is the angle from the ADCP axis to the dam,

U', V', W' are *x*-, *y*- and *z*-velocity components in dam coordinates and,

$\frac{\partial V'_{rms}}{\partial x}, \frac{\partial W'_{rms}}{\partial x}, \frac{\partial V'_{rms}}{\partial y}, \text{and} \frac{\partial W'_{rms}}{\partial y}$ were formed similarly.

Spatial derivatives of velocity with respect to x, y and z were formed from spatial gradients with respect to range. For gradients of velocity with respect to z, the 3-beam solutions were used.

$$\frac{\partial U'}{\partial x} = \frac{\partial U'}{\partial r}\frac{dr}{dx} = \frac{\partial U'}{\partial r}\frac{1}{\cos\theta}$$

$$\frac{\partial U'}{\partial y} = \frac{\partial U'}{\partial r}\frac{dr}{dy} = \frac{\partial U'}{\partial r}\frac{1}{\sin\theta}$$

$\frac{\partial V'}{\partial x}, \frac{\partial W'}{\partial x}, \frac{\partial V'}{\partial y}, \text{and} \frac{\partial W'}{\partial y}$ were formed similarly.

Gradients with respect to *z* incorporated the error velocity, *Er*, described above.

$$\frac{\partial W'}{\partial z} = \frac{\partial V}{\partial z} = \frac{2Er}{\left(\tan 6^\circ\right)^2 \frac{2}{3} r} = \frac{3\ Er}{r\ \left(\tan 6^\circ\right)^2}$$

$$\frac{\partial U}{\partial z} = \frac{Er}{\left(\tan 6^\circ\right)^2 \frac{1}{3} r} = \frac{3\ Er}{r\ \left(\tan 6^\circ\right)^2}$$

$$\frac{\partial W}{\partial z} = \frac{Er}{\frac{1}{3} r \sin 6^\circ} = \frac{3\ Er}{r\ \sin 6^\circ}.$$

Gradient components in the ADCP coordinates need to be recombined to estimate gradients in dam coordinates.

$$\frac{\partial U'}{\partial z} = \frac{\partial U}{\partial z}\sin\theta - \frac{\partial W}{\partial z}\cos\theta \quad \text{and}$$

$$\frac{\partial V'}{\partial z} = -\frac{\partial U}{\partial z}\cos\theta - \frac{\partial W}{\partial z}\sin\theta.$$

ADCP data was averaged over the range extent of the manually tracking box that inscribed the fish in a single ping. These averages were merged with the fish position and tally observations. Spatial and temporal changes of fish positions were calculated using second-order central difference scheme, except for the first and last position changes for a fish event.

Finally, a dataset was formed that included various variables and indices. Indices included the magnitude of root-mean-square velocity (turbulence index), the spatial gradient of velocity (strain index), the time and spatial changes of the turbulence components and fish effort speed.

A.1.5 Observation Visualization

Visualization of fish event pings, water data and other indices and computed variables was performed using the merged database by writing a Tecplot360 software file using a C++ computer program. This file was then loaded into Tecplot360 and contoured and displayed by dam, season and period of the day. All visualizations are presented as two-dimensional Cartesian plots and include an image representing the dam structure.

A.2 Data Analysis

A.2.1 Data Filters

Certain event data, and associated ping observational data, were excluded from the data set to improve the quality of the fish/flow analysis (Table A.1). Overall, 75% of the event and associated ping data were suitable for analysis.

Table A.1. Filters on Event Data. The merged data prior to filtering totaled 50,220 ping observations comprising 4,953 fish events for both dams and seasons combined.

Filter	Exclusion Criterion	Reason	Sequential Number Events Included
Fish speed	> 5 m/s	Biologically realistic	4,949
No. ping to ping observations	< 4 pings per event	Sufficient data for averaging	4,037
Event duration	> 60 sec	No excessive lingering	4,035
Pings outside ADCP/DIDSON overlap zone	> 50% outside	Maximum fish/water synchrony	3,691

A.2.2 Fish Behavior Tallies

To analyze the behavior tally data for schooling and directedness, we reduced the data to percentages of total observations for various subsets. For example, we computed the percentage of school events observed for the subset consisting of the dawn period during spring at McNary Dam. Similarly, the tally data for path of movement was analyzed for percentages of each path for a given subset.

A.2.3 Non-Linear Regression Analysis

Smooth lines were fit using a nonparametric spline routine in SAS software. The procedure used was a method for noisy data (INTERPOL=sm50) which produces a smoothing spline or line describing the relationship between variables. Seber and Wild (1989) give a brief description of smoothing spline approaches to the nonparametric regression problem. As they state, although "a smooth curve can be drawn that goes through all of the data points…we wish to filter out local variability, due to random error from grosser trends." Thus, the purpose of fitting the regression splines is to visualize trends. To avoid

the effect on the regression curve from maximal values of the dependent variable, its upper limit was set at the mean plus the product of 2.57 and the standard deviation.